ICJK
Journal of Advanced Materials Research
http://dx.doi.org/10.62762/JAMR.2026.769952

REVIEW ARTICLE

Hydrogen Storage Behavior of Ti-Based High-Entropy Alloys: A Review

Jingwen Fu[1,†], Junpeng Hu[1,†], Siying Zhang[1,†], Ningyue Sheng[2,†], Tao Lu[1,†], Chenchen Yuan[1,*] and Yao Zhang[1,*]

[1] School of Materials Science and Engineering, Jiangsu Key Laboratory of Advanced Metallic Materials, Southeast University, Nanjing 211189, China
[2] Nantes Université, Ecole Centrale Nantes, CNRS, GeM, UMR 6183, Nantes 44000, France

Abstract

Titanium-based high-entropy alloys (HEAs) have emerged as promising solid-state hydrogen storage materials owing to their structural stability, tunable thermodynamics, and rapid kinetics. This review systematically examines the hydrogen storage behaviour of Ti-based HEAs across three structural categories: body-centered cubic (BCC) single-phase alloys, C14 Laves phase alloys, and multiphase systems containing CsCl-type structures. The high-entropy effect, severe lattice distortion, sluggish diffusion, and cocktail effect collectively enable these alloys to overcome key limitations of conventional materials, including difficult activation, poor reversibility, and insufficient cycling stability. Critical roles of constituent elements—Ti, V, Cr, Zr, Fe, and Mn—in modulating phase stability, hydrogen affinity, and kinetics are discussed. Empirical design parameters such as mixing entropy, valence electron concentration, atomic size mismatch, and electronegativity difference guide composition optimization. Advanced processing techniques, including mechanical alloying, high-pressure torsion, and melt spinning, enhance microstructural control and performance. Recent integration of CALPHAD, density functional theory, and machine learning has accelerated alloy discovery and design. Despite significant progress, challenges persist in balancing capacity with reversibility, mitigating surface oxidation, and ensuring processing consistency. This review provides a comprehensive framework for understanding structure–property relationships in Ti-based HEAs and outlines future directions toward practical hydrogen storage applications.

Keywords: Titanium-based high-entropy alloys, Hydrogen storage, BCC alloys, C14 Laves phase alloys, CsCl-type structures alloys, Structure–property relationships.

Submitted: 04 June 2026
Revised: 08 July 2026
Accepted: 13 July 2026
Published: 03 August 2026

Vol. 2, **No.** 3, 2026.
10.62762/JAMR.2026.769952

***Corresponding authors:**
✉ Chenchen Yuan
yuancc@seu.edu.cn
✉ Yao Zhang
zhangyao@seu.edu.cn

† These authors contributed equally to this work

Citation
Fu, J., Hu, J., Zhang, S., Sheng, N., Lu, T., Yuan, C., & Zhang, Y. (2026). Hydrogen Storage Behavior of Ti-Based High-Entropy Alloys: A Review. *Journal of Advanced Materials Research*, 2(3), 214–235.

1 Introduction

The global transition toward low-carbon energy systems has positioned hydrogen as a key energy carrier owing to its high gravimetric energy density ($120\,\mathrm{MJ\,kg^{-1}}$) and zero carbon emissions [1]. However, the realization of a hydrogen economy is hindered by the limitations of conventional storage technologies. Compressed hydrogen gas (35–70 MPa) is associated with safety concerns and low volumetric energy density, whereas cryogenic liquid hydrogen (≈20 K) requires highly energy-intensive cooling and insulation [2]. In this context, solid-state hydrogen storage in metal hydrides has emerged as a promising alternative, offering higher volumetric density and improved safety under moderate operating conditions [1, 3].

Conventional hydrogen storage research has mainly focused on intermetallic compounds of the AB_2 (Laves phase) and AB_5 types, as well as V-based solid-solution alloys. Among these, Body-Centered Cubic (BCC) V-based alloys are known for their high theoretical hydrogen storage capacities (up to 3.8 wt.%) [1]. However, their practical deployment is limited by difficult activation, sluggish room-temperature kinetics, and pronounced hysteresis [4]. To address these limitations, attention has recently shifted to High-Entropy Alloys (HEAs), also referred to as Multi-Principal Element Alloys (MPEAs), which depart from traditional alloy design by combining five or more principal elements in near-equiatomic ratios [5, 6].

This review examines the hydrogen storage behaviour of Ti-based HEAs. Unlike conventional alloys, HEAs use high configurational entropy to stabilize simple solid-solution phases (BCC or Face-Centered Cubic (FCC)) rather than complex intermetallics, while their characteristic "cocktail effect" and severe lattice distortion enable fine-tuning of thermodynamic and kinetic properties [7, 8]. Recent studies show that Ti-based HEAs can provide reversible hydrogen storage at room temperature, rapid sorption kinetics without prior activation, and excellent cyclic stability, making them promising candidates for next-generation solid-state hydrogen storage materials [9, 10]. In addition, these alloys are being investigated for niche applications such as thermal hydrogen compression [11, 12] and hydrogen isotope separation [13], further highlighting their versatility.

HEAs are defined not only by their nominal composition but also by thermodynamic parameters that govern phase stability. For hydrogen-storage applications, rational design requires balancing capacity (typically favored by BCC phases) and kinetics (often associated with Laves phases). To achieve this, researchers use empirical design parameters in combination with advanced modeling tools such as CALPHAD (CALculation of PHAse Diagrams) and machine learning (ML). A key characteristic of HEAs is their high mixing entropy (ΔS_{mix}), which lowers the Gibbs free energy ($G = H - TS$) and thereby stabilizes disordered solid-solution phases against phase separation [14]. For an equimolar alloy with n elements, ΔS_{mix} is calculated based on Boltzmann's hypothesis:

$$\Delta S_{mix} = -R\sum_{i=1}^{n} c_i \ln c_i, \tag{1}$$

where R is the gas constant and c_i is the atomic fraction. In hexanary systems like Ti-Zr-V-Cr-Ni-Fe, Mishra et al. [15] demonstrated that high entropy is essential for stabilizing single-phase structures at elevated temperatures, preventing the formation of ordered intermetallics that often plague lower-entropy counterparts.

While entropy promotes mixing, the mixing enthalpy (ΔH_{mix}) describes the chemical interaction between constituent elements. Within the framework of the regular solution model, it can be expressed using the Miedema semi-empirical model as:

$$\Delta H_{mix} = \sum_{\substack{i,j=1 \\ i\neq j}}^{n} 4\Delta H_{ij}^{mix} c_i c_j, \tag{2}$$

where c_i and c_j are the atomic fractions of the i-th and j-th elements, respectively, and ΔH_{ij}^{mix} is the binary mixing enthalpy of the i-j pair, which can be calculated from the Miedema parameters of the constituent elements.

In hydrogen storage, ΔH_{mix} influences both the phase stability of the alloy and the metal-hydrogen binding energy [16]. A highly negative ΔH_{mix} typically leads to the formation of intermetallics (like Laves phases), while a positive value promotes phase separation. Recent studies have utilized enthalpy parameters to predict hydride stability in multicomponent Ti-Zr-based systems, enabling the design of alloys with optimized desorption temperatures [17, 18].

Furthermore, the valence electron concentration (VEC) is widely used as a predictor of crystal structure. It is defined as the weighted average of the valence electrons of the constituent elements:

$$VEC = \sum_{i=1}^{n} c_i VEC_i. \quad (3)$$

Empirical guidelines indicate that $VEC < 6.87$ favors BCC structures, whereas $VEC \geq 8.0$ favors FCC structures, as demonstrated in various Ti-based HEA systems [19, 20]. In Ti-based HEAs, low VEC values are targeted to stabilize high-capacity BCC phases [21], while intermediate values (around 6.4) are engineered to promote dual-phase (BCC + Laves) microstructures that provide a compromise between capacity and kinetics [22, 23].

Another critical parameter influencing the chemical bonding characteristics and phase stability of HEAs is the difference in electronegativity ($\Delta\chi$) among the constituent elements. It is calculated as:

$$\Delta\chi = \sqrt{\sum_{i=1}^{n} c_i(\chi_i - \bar{\chi})^2}, \quad (4)$$

where χ_i is the electronegativity of the i-th element. In hydrogen storage materials, $\Delta\chi$ affects the hydride stability. A larger electronegativity mismatch tends to increase the ionic character of the metal-hydrogen bonds, which can lead to excessive stability of the hydride phase, making desorption difficult. Dangwal and Edalati [22] emphasized the importance of $\Delta\chi$ in the design of AB-type HEAs (e.g., $TiV_2ZrCrMnFeNi$), noting that controlling electronegativity differences is essential for ensuring reversibility at room temperature. Similarly, Mishra et al. [15] utilized $\Delta\chi$ as a key descriptor alongside entropy and enthalpy to predict the stability of the C14 Laves phase in Ti-Zr-V-Cr-Ni-Fe alloys. Furthermore, Ma et al. [12] observed that as the V/Fe ratio decreases in Ti-V-Fe-Mn alloys, the average electronegativity increases, which correlates with a decrease in hydride stability and improved desorption properties.

Atomic size mismatch (δ) is another important parameter that quantifies lattice distortion of HEAs:

$$\delta = \sqrt{\sum_{i=1}^{n} c_i \left(1 - \frac{r_i}{\bar{r}}\right)^2}. \quad (5)$$

Large δ values increase lattice distortion and broaden the distribution of interstitial site energies, which can lower the activation barrier for hydride nucleation [25]. Nevertheless, excessive strain, for example, that introduced by severe mechanical deformation in TiZrCrFeMnNi powders, can degrade hydrogen-storage capacity [24].

HEAs are typically defined as alloys containing at least five principal elements, each with an atomic fraction between about 5 and 35 at.%. Beyond this compositional definition, HEAs exhibit four characteristic effects that distinguish them from conventional alloys. These effects are particularly relevant to hydrogen storage, as they influence phase stability, activation kinetics, and thermodynamic properties.

The high-entropy effect is the key thermodynamic feature of HEAs. A large configurational entropy can offset the enthalpy of formation of ordered intermetallic compounds, thereby stabilizing simple solid-solution phases (such as BCC or FCC) at elevated temperatures. In hydrogen storage applications, this effect is exploited to stabilize the high-capacity BCC phase and maintain its structural integrity during repeated hydrogenation-dehydrogenation cycles [15].

Severe lattice distortion arises from the atomic size mismatch (δ) among the constituent elements (for example, mixing large Zr atoms with smaller Fe or Cr atoms), which generates a strained crystal lattice. This distortion is critical for hydrogen storage because it modifies the energy landscape of interstitial sites. A strongly distorted lattice provides a distribution of interstitial site sizes; larger or more weakly bound sites can facilitate hydrogen uptake and diffusion, potentially lowering the activation barrier for hydride nucleation [10]. However, excessive lattice strain, such as that introduced by mechanical deformation in fine powders, can trap hydrogen or reduce the effective reversible capacity, and therefore needs to be carefully controlled [24].

Another characteristic is sluggish diffusion, where the chemically complex local environment in HEAs hinders cooperative atomic diffusion, leading to exceptional thermal stability and resistance to grain coarsening. This sluggish diffusion is beneficial for retaining nanostructured features (such as those produced by mechanical alloying or melt spinning) at operating temperatures, which is important for maintaining fast hydrogen sorption kinetics over long-term cycling [9, 25].

Finally, the cocktail effect refers to the synergistic

combination of multiple elements, where the overall properties are not a simple linear average of the individual components. In Ti-based HEAs, this effect enables the simultaneous optimization of otherwise competing properties: additions of Zr and V primarily enhance hydrogen storage capacity (structural role), while additions of Fe and Ni promote hydrogen dissociation and destabilize the hydride, improving room-temperature reversibility (functional role) [21, 26].

The complexity of the HEA compositional space renders trial-and-error inefficient. Recent advancements have successfully integrated Machine Learning (ML) with CALPHAD and Density Functional Theory (DFT) to accelerate materials discovery. Enblom et al. [27] employed ML to identify interstitial volume as a key descriptor for hydride stability in Ti-Zr-Mn-Cr-Fe-Ni Laves phases. Edalati et al. [17] combined ML with thermodynamic calculations to predict the enthalpy of hydride formation for Ti-Zr-Mn-Fe-Co alloys with high accuracy. First-principles calculations by Shen et al. [28] revealed that hydrogen prefers tetrahedral sites in BCC lattices and that hydrogenation can degrade mechanical properties (bulk and shear modulus) in TiZrHfMoNb alloys. Additionally, CALPHAD is widely used to predict phase equilibria, such as the coexistence of BCC and C14 phases in Ti-V-Nb-Cr systems [7] and the phase stability of Ti-Zr-Ni-Fe-V systems [29]. These computational and data-driven approaches have thus become indispensable tools for designing Ti-based HEAs with targeted hydrogen storage properties.

Research on HEAs for hydrogen storage has expanded rapidly worldwide and now covers Mg-based, Ti-based, and other refractory alloy systems. Mg-based materials are traditionally valued for their high gravimetric hydrogen capacity ($7.6\,\mathrm{wt\%}$ for MgH_2). In HEA-based design, the high-entropy effect is exploited to weaken the strong Mg–H bonds and improve sorption kinetics. Although fully Mg-based HEAs are less common than transition-metal HEAs because of the volatility of Mg, substantial progress has been made in using HEAs as catalysts in Mg-based systems. Wei et al. [6] synthesized a $(TiVZrNb)_{38}Cr_{17}$ HEA and employed it as a catalyst for MgH_2. During cycling, the BCC→FCC phase transformation in the HEA created additional diffusion pathways, markedly enhancing the hydrogen absorption/desorption kinetics of MgH_2 and lowering the activation energy, illustrating the potential of HEAs to enhance conventional hydrogen storage materials.

However, refractory Ti-based HEAs have attracted considerable attention because they form hydrides with high capacity and favorable thermodynamics near room temperature. Unlike Mg-based systems, Ti-based HEAs typically form BCC or Laves phases that operate under relatively moderate conditions. The BCC phase is attractive because its open lattice can accommodate hydrogen contents up to $H/M \approx 2$, and single-phase BCC HEAs such as Ti–V–Cr–Mn–Nb exhibit capacities of approximately 3.45 wt% [32]. However, pure BCC alloys often display sluggish activation due to the formation of passivating oxide layers [25]. For example, Ti–Zr–Hf–Mo–Nb alloys require elevated temperatures for hydrogen absorption [30]. Savvotin et al. [31] mitigated this issue by applying a Pd coating, which enabled room-temperature absorption in Ti–Zr–V–Nb–Ta. Similarly, Liu et al. [32] reported that Ti–V–Cr–Mn–Nb alloys can reach capacities of approximately 3.45 wt% with good reversibility.

Conversely, Laves phases (C14/C15) generally show excellent activation and fast kinetics but lower hydrogen capacities. Many Ti-based HEAs spontaneously form Laves phases when elements with large atomic radius differences are combined. The equiatomic TiZrVCrNi alloy, for instance, forms a single C14 phase with rapid kinetics but a limited capacity of $1.6\,\mathrm{wt\%}$ [33]. Likewise, Ti–Zr–Cr–Mn–Fe–Ni alloys designed using specific valence electron concentration (VEC) criteria form C14 phases that are fully reversible at room temperature [22, 23]. In these systems, the Laves phase acts as a "catalytic gateway," facilitating H_2 dissociation [34]. Mishra et al. [15] further reported single-phase C14 Laves phases in Ti–Zr–V–Cr–Ni–Fe, demonstrating their high-temperature stability.

Combining the high capacity of BCC phases with the fast kinetics of Laves phases emerged as a widely adopted design strategy. In such dual-phase microstructures, the Laves phase catalyzes surface H_2 dissociation, whereas the BCC phase serves as the main hydrogen reservoir. Marques et al. [61] and Vicente et al. [29] showed that in Ti–Zr–V–Fe–Ni systems, the C14 phase controls activation, while the BCC phase provides enhanced capacity. Compositional tuning is crucial; for instance, in $(TiVZrNb)_{1-x}Fe_x$ alloys, increasing the Fe content promotes the formation of the C14 phase, and an optimized composition delivers a capacity of ~ 3.19 wt% [35, 36]. Similarly, Zareipour et al. [33] achieved

a total hydrogen absorption of ~ 2.3 wt% in TiVCrFeZr by designing a microstructure in which a BCC phase is embedded in a continuous Laves network, although the reversible capacity was approximately 1.0 wt%. Wang et al. [37] proposed a "binding-energy crossover" mechanism in TiZrCrMnNi(VFe), whereby lattice strain originating from the Laves phase reduces the hydrogen binding energy in the BCC phase, thus facilitating low-temperature desorption.

The compositional flexibility of Ti-based HEAs enables fine-tuning of hydrogen storage properties through targeted elemental substitutions, known as the "cocktail effect". Zirconium (Zr) is a strong stabilizer of the C14 Laves phase. In Ti–V–Cr–Nb–Zr alloys, increasing the Zr content raises the Laves-phase fraction and the plateau pressure, thereby improving reversibility [36]. In Ti–Zr–Fe–Mn–Cr–V systems, higher Zr contents enhance both cycle life and thermodynamic characteristics [38, 39]. Iron (Fe) generally destabilizes hydrides and lowers desorption temperatures. Cheng et al. [40] reported a complex trade-off: small Fe additions improve surface catalysis, whereas excessive Fe introduces lattice strain that compromises mechanical stability. Nickel (Ni) tends to segregate to the Laves phase, where it acts as an efficient catalyst. In Ti–Cr–Mo alloys, Ni additions promote the precipitation of a secondary phase that effectively eliminates incubation time [13]. Vanadium (V) is essential for stabilizing the BCC phase. Chen et al. [26, 38] showed that partial substitution of V with Fe, Mn, or Cr significantly improves plateau flatness.

Multi-scale characterizations coupling in-situ neutron diffraction, DFT first-principles calculations and CALPHAD thermodynamic simulations further uncover the fundamental mechanisms behind the superior hydrogen storage capability of Ti-based HEAs. Hu et al. [41] utilized DFT calculations on TiZrHfMoNb to quantify metal-hydrogen binding energy, radial distribution function and phonon spectra, and confirmed that intrinsic severe lattice distortion unique to high-entropy matrices diversifies interstitial energy levels and lowers hydrogen migration barriers, which differs fundamentally from conventional BCC pure metals. Montero et al. [42] adopted in-situ neutron diffraction on $Ti_{0.30}V_{0.25}Zr_{0.10}Nb_{0.25}Ta$ refractory HEA to track real-time lattice structural evolution during dehydrogenation, and validated the single-step reversible BCC-to-FCC phase transition accompanied by hydrogen occupation shift from octahedral to tetrahedral interstitial sites at the critical hydrogen concentration of 1.08 wt%. Andrade et al. [43] performed CALPHAD thermodynamic simulations combined with X-ray Rietveld refinement on equiatomic TiZrNbCrFeNi AB-type HEA, which precisely predicted the competitive formation of dual C14 Laves phases and clarified how adjustable valence electron concentration mediates hydride formation enthalpy and room-temperature sorption reversibility. The complementary experimental and computational results from these three characterization techniques jointly interpret the origin of outstanding hydrogen storage performance in Ti-based HEAs: the cocktail effect tunes metal-hydrogen bonding strength, inherent lattice distortion supplies abundant interstitial storage sites, and reversible phase transformation guarantees cyclic hydrogen uptake and release under mild conditions.

Advanced processing techniques are also critical for optimizing these materials. Mechanical Alloying (MA) generates nanocrystalline structures with a high density of grain boundaries that enhance hydrogen diffusion. Singh et al. [20], Lee et al. [25] and Zhai et al. [8, 44] showed that MA-synthesized Ti–Fe–Co–Ni–Cu and Ti–V–Cr–Mn–Fe alloys activate much more readily than their as-cast counterparts. High-Pressure Torsion (HPT) involves severe plastic deformation that introduces a very high dislocation density. Hidalgo-Jimenez et al. [39] demonstrated that HPT-processed Ti–Zr–Mn–Fe–Cr alloys activate immediately at room temperature, even after several months of air exposure. Melt Spinning allows for rapid solidification; Kumar et al. [9, 45] reported that melt-spun TiZrVCrNi ribbons exhibit higher capacities ($2\,\mathrm{wt}\%$) and superior kinetics compared with bulk alloys, owing to their refined C14 microstructure. Additionally, Additive Manufacturing methods like Laser Engineered Net Shaping (LENS) allow for the synthesis of complex geometries. Kunce et al. [46] and Tau et al. [47] used LENS to synthesize Ti–Zr–Nb–Mo–V and Ti–V–Cr–Fe alloys, achieving unique non-equilibrium microstructures, although chemical homogeneity remains a challenge to be optimized.

Beyond their role in solid-state hydrogen storage, Ti-based HEAs are also being investigated for other energy-related functions. Wei et al. [6] demonstrated that (TiVZrNb)Cr HEAs can serve as efficient catalysts for MgH_2 storage, and isotope effects in TiZrHfNbTa have been examined for deuterium separation [29]. In summary, Ti-based HEAs constitute a versatile platform for hydrogen storage. By tailoring the

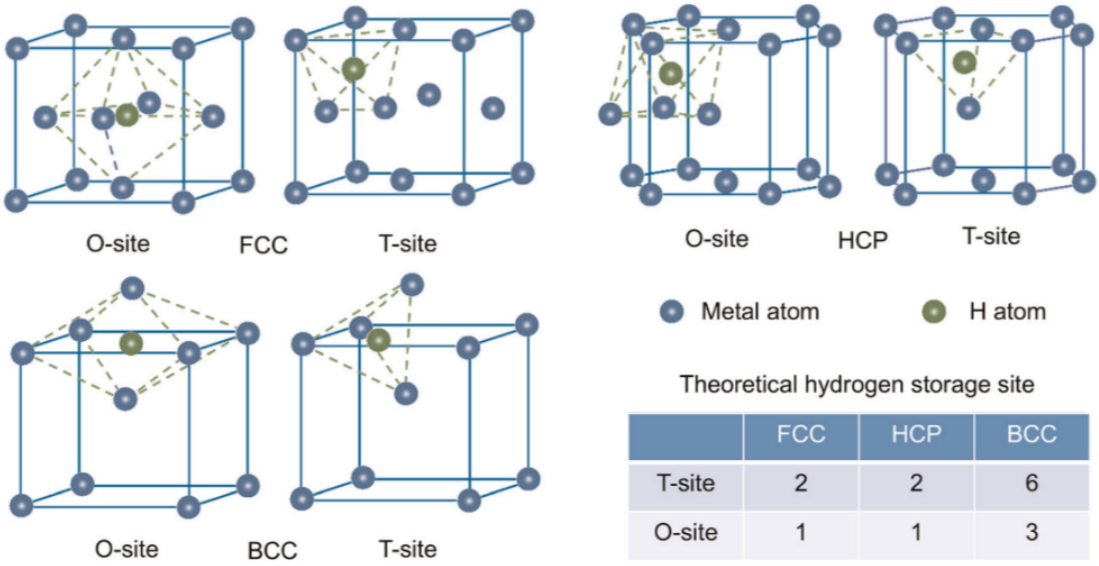

Theoretical hydrogen storage site

	FCC	HCP	BCC
T-site	2	2	6
O-site	1	1	3

Figure 1. Theoretical hydrogen storage sites of FCC, HCP and BCC structures.

elemental composition and employing advanced processing routes, recent studies have begun to overcome several limitations of conventional alloys. The following sections provide a detailed discussion of the specific alloy systems considered in this review.

2 Ti-based BCC HEAs

Body-centered cubic (BCC) high-entropy alloys (HEAs) have long been considered as one of the most promising solid-state hydrogen storage materials due to the intrinsically high hydrogen solubility and fast diffusion kinetics. Studies have confirmed that hydrogen storage alloys form interstitial hydrides when reacting with hydrogen, with hydrogen typically occupying tetrahedral or octahedral interstitial positions within the alloy [48]. Various metal lattices, including face-centered cubic (FCC) [49], BCC [50] and hexagonal close-packed (HCP) [51], are commonly found. The position of hydrogen within these lattices determines the number of hydrogen atoms that an alloy with a specific crystal structure can accommodate. In FCC structures, one hydrogen atom can be accommodated in an octahedral position and two in tetrahedral positions within each unit cell. Similarly, one octahedral position and two tetrahedral positions can be filled in the HCP structure per unit cell (Figure 1 [1]).

Driven by these advantages, a wide range of BCC HEAs, such as TiZrNbHfTa [52], TiZrNbTa [53], TiVZrNbTa [31], and TiZrHfMoNb, have been systematically investigated and consistently exhibit relatively high hydrogen capacities combined with fast absorption and desorption kinetics. These findings collectively establish the BCC phase as the structural cornerstone for Ti-based HEA hydrogen storage materials.

2.1 Roles of Ti, V, and Cr in BCC HEAs

Within Ti-based BCC hydrogen storage alloys, Ti and V are commonly used as base elements because of their high gravimetric hydrogen capacities and good mutual solubility, which promote the formation of a stable BCC solid-solution matrix. This BCC framework offers abundant interstitial sites and continuous diffusion pathways, providing a favorable kinetic basis for hydrogen uptake. However, Ti-rich or binary Ti-V alloys tend to form overly stable hydrides, resulting in sluggish desorption and limited reversibility under practical conditions.

To address this issue, the introduction of a third alloying element is essential for thermodynamic regulation, with Cr playing a key role in Ti-V-Cr systems. Although Cr contributes little directly to hydrogen capacity, it stabilizes the BCC phase and adjusts the valence electron concentration, thereby weakening metal-hydrogen interactions, increasing plateau pressure, and improving kinetics and cycling stability. Consequently, a clear functional synergy is established in Ti-V-Cr alloys, where Ti provides hydrogen affinity, V ensures BCC stability and diffusion, and Cr serves as a thermodynamic and kinetic regulator. Extension of this synergistic design to high-entropy and multi-principal-element alloy frameworks further broadens the compositional space for tuning hydrogen storage performance.

2.2 Hydrogen storage in Ti-V-Cr BCC HEAs

Early exploration of high-entropy effects in hydrogen storage alloys can be traced back to the work of Kao et al. [14] in 2010, who reported hydrogen absorption in $CoFeMnTi_xV_yZr_z$ alloys. In that study, the high configurational entropy was shown to stabilize a single-phase structure and enhance hydrogen storage performance through compositional optimization of Ti, Zr, and V.

Subsequent studies further clarified the unique potential of HEAs in hydrogen storage by fabricating TiZrNbMoV alloys using Laser Engineered Net Shaping (LENS) combined with laser remelting [46]. This processing route yielded dense and chemically homogeneous microstructures, enabling a maximum hydrogen storage capacity of approximately 2.3 wt%. These results demonstrated that the high-entropy concept could be successfully integrated with advanced manufacturing techniques to produce structurally robust hydrogen storage materials.

Beyond bulk storage, Ti-Cr-V HEAs have also been explored as functional catalysts in composite hydrogen storage systems. For example, an MgH_2-based composite incorporating $(TiVZrNb)_{83}Cr_{17}$ HEA as a catalytic additive showed markedly enhanced absorption and desorption kinetics [6]. The improvement was attributed to the combined effects of the high-entropy "cocktail effect" and severe lattice distortion, which promote H_2 adsorption/dissociation and accelerate hydrogen diffusion. Moreover, the intrinsic structural stability and reversible (de)hydrogenation behavior of the HEA were proposed to improve the overall reversibility and cycling durability of the composite system.

Notably, the role of Cr in certain HEA systems has been shown to be dominated by surface effects rather than bulk diffusion [10]. Phase-decoupled control experiments and X-ray photoelectron spectroscopy analyses revealed that Cr-enriched complex oxide layers formed on FCC phases can serve as highly active catalytic surfaces. In such cases, rapid hydrogen uptake at room temperature under relatively low pressure is governed primarily by facilitated H_2 dissociation and surface penetration, rather than by hydrogen diffusion through the bulk lattice.

2.3 Regulation Strategies for Ti-Cr-V BCC hydrogen storage HEAs

In recent years, research on Ti-Cr-V BCC HEAs and multi-principal-element hydrogen storage alloys has progressively shifted from material discovery toward rational and controllable design. Performance optimization is generally achieved through several interrelated regulatory strategies, as summarized below.

2.3.1 Composition and Thermodynamic Regulation

In Ti-V-Cr based high entropy and multi principal element hydrogen storage alloys, research has commonly started from compositional design, because elemental ratios simultaneously modulate lattice volume, valence electron concentration, and hydrogen metal bonding strength, thereby governing hydride stability and the plateau pressure in pressure composition isotherms. Accordingly, by introducing or tuning elements such as Mn, Fe, Mo, and Al, overly stable hydrides can be destabilized and the plateau pressure can be shifted upward or adjusted to move absorption and desorption toward an ambient temperature operating window; meanwhile, the structural stability of the BCC matrix must be retained to avoid capacity loss. In parallel, these studies have typically distinguished maximum hydrogen uptake from practically reversible hydrogen release, emphasizing that high uptake can be translated into high usable capacity only when the thermodynamic driving force and plateau pressure match the relevant engineering pressure range. This perspective has led to a composition window based design logic that balances capacity, hysteresis, and reversibility.

2.3.2 Phase Structure and Interface Regulation

After thermodynamic optimization has established the basis for reversibility, attention has increasingly shifted to phase architecture and interface engineering, because performance improvements in Ti-V-Cr systems are often constrained by first hydrogenation activation and diffusion kinetics. Accordingly, dual phase or multiphase microstructures, such as BCC plus C14 Laves or BCC plus FCC, have been constructed to exploit phase boundaries as defect-rich regions and short-range diffusion pathways, thereby lowering nucleation barriers and shortening the incubation period to enable rapid hydrogen uptake under relatively mild conditions [54, 55]. In parallel, the introduction of a secondary phase can not only improve kinetics and activation behavior but also regulate the hydrogenation pathway and the sequence of phase transformations, giving rise to a cooperative mechanism in which a kinetically fast phase facilitates initiation while the BCC phase provides the primary storage capacity. Nevertheless, because secondary

phases may reduce the number of available interstitial sites or introduce irreversible hydrogen trapping, this strategy requires precise control over phase fraction and phase stability to achieve a quantifiable trade-off between capacity and kinetics.

2.3.3 Surface Catalysis and Activation Regulation

However, even when an alloy is engineered to exhibit an application-relevant thermodynamic window and a favorable multiphase architecture, Ti-Cr-V-based systems can still underperform in practice because the rate-controlling step often shifts to surface activation, where dense oxide films hinder H_2 dissociation and the subsequent injection of H atoms into the lattice [56]. Consequently, recent Ti-Cr-V studies increasingly treat the surface not as a passive "contaminant layer" but as an actively tunable component of the storage material [2]. One effective approach is chemical activation by targeted additions. For instance, rare-earth alloying (e.g., Ce) has been shown to modify both the chemistry and defect structure of surface oxides, so that the first hydrogenation proceeds under markedly milder conditions; in Ti-V-Cr-Mn-Mo-based alloys, a small Ce addition can shorten the incubation period and enable hydrogen uptake at room temperature without the severe pre-activation typically required for this family [2]. A complementary strategy is to introduce Ni-containing secondary phases (such as Zr-Ni additives), which provide catalytically active sites for H_2 dissociation and create fresh, permeable metal/oxide interfaces during cycling; in representative Ti-V-Cr alloys, such additives compress incubation from the order of hours to the order of minutes while maintaining multi-wt% hydrogen uptake [57]. Beyond direct alloy design, Ti-V-Cr-related high-entropy phases can also serve as interfacial catalysts in composite hydrides, where the surface limitation is transferred from the alloy to the hydride interface. Notably, incorporating a Ti-V-(Nb/Zr)-Cr HEA into MgH_2 markedly lowers the dehydrogenation onset (to below 500 K), accelerates release kinetics to near-complete desorption at elevated temperature, and improves cycling retention, consistent with a combined effect of catalytic dissociation, fast diffusion pathways, and sustained interfacial reactivity [6, 58]. Taken together, these results establish that surface chemistry is a designable functional layer; once surface activation is secured, the intrinsic thermodynamic and transport advantages of the BCC-based bulk can be fully exploited, enabling faster and more reversible hydrogen storage at or near room temperature.

2.3.4 Processing and Fabrication Regulation

Beyond compositional design, phase architecture, and surface activation, processing and post-treatment offer a decisive route to improve practical hydrogen storage performance because they concurrently tune grain size, defect density, and the spatial distribution of the BCC matrix and secondary phases, thereby shortening diffusion distances and increasing reactive interfaces. Mechanical alloying is particularly effective: the high density of defects and nanocrystalline BCC domains lowers activation barriers and accelerates room-temperature kinetics [59]; for instance, in mechanically alloyed Ti-V-Cr-Mn-Fe alloys, appropriate Mn/Cr tuning can raise the room-temperature capacity from 1.08 to 1.39 wt% while reducing the onset temperature for hydrogen uptake. Heat treatment can further relieve internal stresses and stabilize phase constitution, yet it may also redistribute phase fractions and trigger transformations that reshape both capacity and reversibility. In some systems, annealing removes incubation but causes capacity losses when the BCC reservoir is consumed by phase redistribution, whereas in others it increases capacity (up to 2.34 wt%) and reduces the apparent activation energy (from 83.30 to 66.26 kJ mol^{-1}) by optimizing hydride stability and transport pathways. Nevertheless, processing remains a double-edged lever, as excessive phase separation or brittle phase formation can reduce maximum capacity and accelerate degradation. Therefore, processing parameters should be co-designed with the phase-stability window, interface density, and surface state so that the BCC phase retains its capacity potential while faster kinetics and longer cycle life are achieved.

2.3.5 Simulation and Computation Driven Regulation

Employing experimental techniques in the search for the most suitable high entropy alloys (HEAs) with improved hydrogen storage properties demands enormous efforts and can be costly. The use of empirical and thermodynamic modelling and simulation have proven to be very efficient methods to overcome the enormous effort required to find new HEAs and explore their wide compositional space, due to their ability to predict the desired properties and phase of HEAs for hydrogen storage [60–62].

In Ti-V-Cr based BCC hydrogen storage materials, modelling has increasingly shifted from post hoc interpretation to a priori screening and has been coupled with experiments in a closed loop [63–65].

CALPHAD thermodynamic modelling, supported by continuously improved databases, enables phase equilibria to be predicted in multicomponent systems (for example, Ti-V-Fe-Mn) and clarifies competition between a BCC matrix and secondary phases such as C14 Laves, thereby linking composition, phase constitution, and lattice parameters to hydrogen storage behaviour while reducing trial and error [65]. To enhance reliability, first principles formation enthalpies have been incorporated into parameter assessment, improving predictions of as-cast phase constitution and processing windows. At the atomic scale, density functional theory provides mechanistic guidance on hydrogen site occupancy, phase transition thresholds, capacity limits, and dehydrogenation trends; for TiZrVMoNb, for instance, a BCC to FCC transformation has been predicted near $1.5\,\mathrm{wt\%}$ H, together with occupancy preferences and an estimated upper capacity of $2.65\,\mathrm{wt\%}$, offering quantitative targets for compositional tuning. In parallel, descriptor based frameworks using valence electron concentration, atomic size mismatch, and electronegativity difference have been applied to screen candidates for near room temperature reversibility, as exemplified by TiVZrCrMnFeNi [66, 67]. Importantly, these calculations have been integrated with thermodynamic and operando measurements, including Tian Calvet calorimetry to track reaction enthalpy versus H/M and in situ X-ray diffraction to resolve transformation sequences, while surface activation strategies such as Pd catalytic layers have enabled room temperature first hydrogenation [68, 69]. Collectively, this computation-mechanism-design paradigm aligns with broader consensus in high entropy hydrogen storage, where lattice distortion has been associated with increased uptake (for example, $2.5\,\mathrm{H/M}$ in TiVZrNbHf) and where phase stability, site occupancy, and plateau pressure are increasingly treated as computable screening criteria for predictive alloy discovery [70].

The hydrogen absorption and desorption behaviour of Ti-V-Cr based BCC high entropy and multi-principal element alloys is not governed by a single factor; rather, it is controlled by the interplay among the thermodynamic window, phase architecture with interfacial transport, and activation of the surface oxide layer. Compositional design determines hydride stability and the plateau pressure position, secondary phases and defect networks provide short-range diffusion pathways [22], and reactive surface oxides often set the threshold for first hydrogenation while strongly influencing reversibility [71].

3 Ti-based HEAs with C14 Laves phase

3.1 Intrinsic Characteristics and Hydrogen Storage Potential of Titanium-Based C14 Laves Phase

The C14 Laves phase is a classic structural phase in the field of hydrogen storage, belonging to the hexagonal crystal system and possessing a large number of tetrahedral interstitial sites. Compared to BCC phase alloys (with hydrogen storage capacities in the range of 3.8 to 4 wt.%), its inherent hydrogen storage capacity is not high (only 1.5–1.8 wt.%), but it can significantly improve the hydrogen absorption/desorption kinetics of alloys. It often exists as a second phase within the BCC phase, providing diffusion channels for hydrogen atoms to rapidly enter the main BCC phase. Among them, $TiMn_2$-based C14 Laves phase alloys are known for their easy activation and favorable kinetics [72]. However, binary $TiMn_2$ alloys are limited by excessively high equilibrium plateau pressures and poor cycling stability for practical applications [73].

3.2 Experimental Progress in Ti-Mn-Based Laves Phase High-Entropy Alloys

In the design of traditional Ti-Mn-based Laves phase alloys, Ti, as a strong hydride-forming element, provides the alloy's fundamental affinity for hydrogen and determines the upper limit of theoretical hydrogen storage capacity. Mn, on the other hand, preliminarily adjusts the plateau pressure by regulating the unit cell volume. However, the simple Ti-Mn binary combination struggles to achieve precise thermodynamic balance for hydrogen absorption and desorption. Consequently, multiple elements are introduced to form a high-entropy system for fine-tuning: Ti/Zr provides hydrogen affinity and unit cell size control, Mn ensures the stability of the Laves phase matrix, and elements like Cr serve as thermodynamic fine-tuning agents.

Within the $TiMn_2$ system, alloys designed based on the high-entropy concept can be mainly categorized into two types. One type retains the C14 Laves phase structure while introducing various elements for adjustment, optimizing performance via the cocktail effect, such as the Ti-Zr-Cr-Mn-Fe-Ni system. The other type involves multi-phase composites, forming complex structures like C14+BCC or C14+FCC, leveraging the synergistic effects of multiple phases to optimize performance.

3.2.1 *High-Entropy Laves Phase Alloys*

Considering three criteria—VEC = 6.4, single-phase thermodynamic stability, and AB_2H_3 hydride formation—Edalati et al. [23] designed the high-entropy alloy TiZrCrMnFeNi for reversible room-temperature hydrogen storage. The alloy was prepared using arc melting under an argon atmosphere (remelted 6 times to ensure compositional homogeneity). Characterization revealed its primary phase to be 95 wt.% C14 Laves phase (hexagonal, $P6_3/mmc$, $a = 0.493\,\mathrm{nm}$, $c = 0.809\,\mathrm{nm}$), containing only a small amount of a Ti/Ni-enriched cubic phase (Pm-3m, $a = 0.305\,\mathrm{nm}$). The C14 phase consisted of coarse grains several hundred micrometers in size, while the cubic phase was dispersed with fine morphology within the C14 grains and at grain boundaries. Experimental results demonstrated that TiZrCrMnFeNi possesses excellent kinetic properties and cycling performance, capable of reversible hydrogen absorption and desorption at room temperature without activation, achieving 1.7 wt.%.

3.2.2 *High-Entropy Multiphasic Alloys*

Zhai et al. [44] systematically investigated the influence of Mn/Cr ratio adjustment on the phase structure and hydrogen storage properties of $Ti_{35}V_{35}Cr_{20-x}Mn_{5+x}Fe_5$ system high-entropy alloys prepared by mechanical alloying. As shown in Figure 2, they found that with increasing Mn content, the lattice distortion and formation enthalpy of the alloys decreased, and the formation of the C14 Laves phase (AB_2-type hexagonal structure) was significantly suppressed. The proportion of the BCC phase and its lattice constant increased. Conversely, increasing Cr content promoted the formation of the Laves phase while also increasing lattice distortion. Mechanical alloying produced a nanocrystalline structure in the alloys, with uniformly distributed elements and no segregation. The grain size decreased as lattice distortion increased. Increasing Mn content significantly enhanced the room-temperature hydrogen storage capacity of the alloys, from 1.08 wt.% for $Cr_{20}Mn_5$ to 1.39 wt.% for Cr_5Mn_{20}. This is attributed to the increased proportion of the BCC phase (which has a much higher theoretical hydrogen storage capacity than the Laves phase) and lattice expansion, which provides more space for accommodating hydrogen atoms. It can be seen that under the composite effect of BCC and C14 Laves phases, the alloys not only maintain relatively fast hydrogen absorption/desorption kinetics but also achieve a considerable improvement in hydrogen storage capacity.

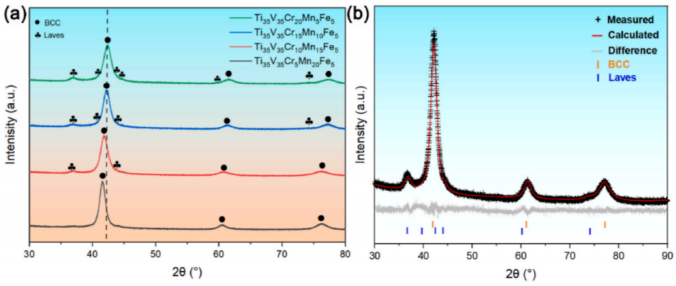

Figure 2. (a) XRD patterns of the as-milled $Ti_{35}V_{35}Cr_{20-x}Mn_{5+x}Fe_5$ ($x = 0, 5, 10, 15$) HEAs; (b) Rietveld refinement of representative $Ti_{35}V_{35}Cr_{20}Mn_5Fe_5$ HEA [44].

3.3 Regulation Strategies for $TiMn_2$-Based Laves Phase High-Entropy Alloys

In recent years, research on $TiMn_2$-based Laves phase high-entropy alloys has shifted from simple phase formation exploration to directional performance optimization. The regulatory strategies primarily revolve around the following levels.

3.3.1 *Composition Design*

In Ti-Mn-based Laves phase high-entropy alloys, composition design directly determines the stability of the hydrides. Because the Laves phase structure is extremely sensitive to the atomic radius ratio (R_A/R_B), systematically adjusting the elemental ratios at the A-site (Ti, Zr, potentially introduced Y or rare-earth elements) and B-site (Mn, Cr, V, Fe, Mo) can control the unit cell parameters and electron concentration. Studies have concluded that substituting Zr for Ti and V for Mn leads to an almost linear increase in unit cell volume with the substitution amount and A-site hyper-stoichiometry, resulting in increased hydrogen storage capacity and a corresponding decrease in the hydrogen desorption plateau pressure [21]. Furthermore, the dehydrogenation enthalpy and entropy of hydrogen are significantly affected by the substitution of Mn with V, thereby improving the dehydrogenation performance at room temperature. In $Ti_{0.84}Zr_{0.16}Mn_{0.9-x}Cr_{0.7}Fe_{0.1}$ ($x = 0, 0.1, 0.2$) and $Ti_{0.84}Zr_{0.16}Mn_{0.9}Cr_{0.7-y}Fe_{0.1}$ ($y = 0, 0.1, 0.2, 0.3$) alloys, as the Mn, Cr content, or the Mn/Cr ratio increases, the unit cell volume of the C14 phase decreases. The material's hydrogen storage capacity decreases, the equilibrium hydrogen absorption/desorption pressure increases, and the plateau phase slope decreases. This demonstrates that a lower Mn/Cr ratio helps reduce the plateau

pressure [74]. Additionally, excess Zr or Ti, while potentially increasing capacity, may lead to overly stable hydrides, reducing reversible capacity. Therefore, the current research focus is on finding a "compositional window" within which the alloy can leverage both the intrinsic high stability of the Laves phase and the continuous tunability of plateau pressure brought about by lattice distortion from the high-entropy effect. This aims to convert the maximum hydrogen storage capacity into effective reversible capacity under practical operating conditions.

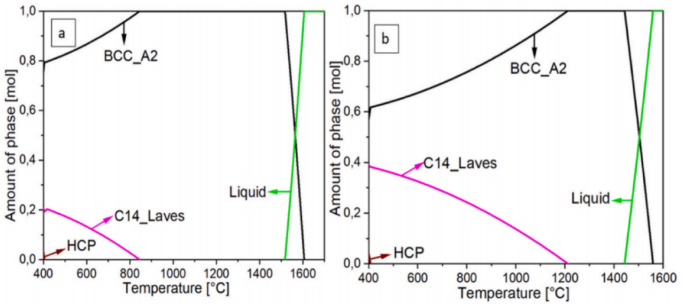

Figure 3. Phase diagram of (a) $Ti_{32}V_{32}Nb_{18}Cr_9Mn_9$ and (b) $Ti_{27.5}V_{27.5}Nb_{20}Cr_{12.5}Mn_{12.5}$ calculated by the CALPHAD method using Thermo-Calc software (TCHEA7 database) [75].

3.3.2 *Phase Structure Regulation*

Although single-phase Laves alloys exhibit good kinetic properties, their theoretical hydrogen storage capacity is generally lower than that of BCC-structured alloys. To overcome this capacity bottleneck, researchers have adopted the design concept of introducing a C14 Laves phase into Ti-V-Cr BCC alloys, and incorporated the BCC phase into Ti-Mn-based alloys to construct BCC + Laves dual-phase or multi-phase structures [75]. In this design, the BCC phase serves as a high-capacity "hydrogen storage reservoir," providing the primary space for hydrogen storage, while the C14 Laves phase acts as a "kinetic window." Due to its easy activation and high hydrogen diffusion coefficient, it preferentially absorbs hydrogen and undergoes volume expansion. The resulting stress field and phase interface defects can "awaken" the BCC phase, enabling it to rapidly absorb hydrogen under mild conditions. This synergistic mechanism at the phase interfaces often results in dual-phase alloys exhibiting superior comprehensive performance compared to single BCC or single Laves alloys [76]. However, the Laves phase, as a topologically close-packed phase, is inherently brittle and can be a source of hydrogen embrittlement. Therefore, precise control of the volume fraction, distribution state, and coherency relationship of the second phase with the BCC matrix is key to achieving a "win-win" scenario for both capacity and kinetics. As shown in Figure 3, Serrano et al. [75] used the CALPHAD method to predict the phase equilibrium of Ti-V-Nb-Cr-Mn high-entropy alloys for hydrogen storage. The calculated phase diagrams demonstrate that both the Cr/Mn ratio and heat treatment temperature can precisely regulate the precipitation fraction and formation temperature range of the BCC phase and Laves phase.

3.3.3 *Surface and Catalytic Regulation*

Ti-Mn-based alloys, especially those containing high proportions of Ti and Zr, readily form dense oxide layers (TiO_2, ZrO_2) on their surfaces. This passivation film is the primary obstacle to initial hydrogen absorption (activation). Even if the alloy interior possesses the optimal thermodynamic window and phase structure, its hydrogen storage performance cannot be realized if hydrogen molecules cannot be effectively dissociated and injected at the surface. Therefore, surface catalytic regulation is crucial.

An effective strategy is the introduction of catalytically active elements. For example, adding trace amounts of Pd, Ni, or rare-earth elements (such as La, Ce) to Ti-Mn-Cr-V alloys. Rare-earth elements can react with the surface oxide layer, generating rare-earth oxides with oxygen vacancies. These defect sites can serve as active centers for hydrogen molecule dissociation, significantly reducing activation temperature and time.

3.3.4 *Preparation Processes*

Preparation processes are core methods for regulating the phase composition, microstructure, and hydrogen storage/mechanical properties of $TiMn_2$-based high-entropy alloys. Vacuum arc melting and induction melting are common laboratory methods for preparing bulk materials. Through inert atmosphere protection, multiple remelts, and water-cooled rapid solidification, they can effectively suppress Mn volatilization and elemental segregation, promote the formation of a single C14 Laves phase, and reduce the precipitation of brittle impurity phases.

Furthermore, Ha et al. [24] prepared a TiZrCrFeMnNi high-entropy alloy via vacuum arc melting and studied the effect of different particle sizes on its hydrogen storage properties after manual crushing. Powder metallurgy processes, such as mechanical

alloying, achieve alloying in the solid state by adjusting parameters like milling time and ball-to-powder ratio. They can effectively introduce lattice distortion and obtain nanocrystalline or amorphous structures, significantly enhancing the kinetic properties of hydrogen diffusion, but require balancing the contradiction between grain refinement and impurity introduction [77]. Heat treatment processes, including homogenization annealing and solution treatment, serve as key bridges connecting preparation and performance. Through precise control of temperature and time, they can eliminate internal stress, stabilize the primary phase (e.g., Laves phase), and suppress the precipitation of unfavorable secondary phases. In summary, the preparation of high-entropy alloys is a multi-scale, multi-objective systems engineering task. It requires the flexible selection and combination of processes based on performance requirements (such as high capacity, fast kinetics, or easy activation) to ultimately achieve the synergistic optimization of composition, structure, and properties.

4 Ti-based HEAs with CsCl-Type Structure

4.1 Intrinsic Properties and Hydrogen Storage Potential of CsCl-Type Structure in Ti-Based High-Entropy Alloys

4.1.1 Crystal Structure of the CsCl-Type Phase

The CsCl-type phase is an important phase structure in the field of hydrogen storage, belonging to the cubic crystal structure with a space group of Pm-3m. It commonly exists in TiFe alloy. In this structure, Ti atoms and Fe atoms occupy the vertex and body-centered positions of the unit cell, respectively, forming an ordered arrangement. There are three types of octahedral interstitial sites and six types of tetrahedral interstitial sites within the unit cell, which serve as the main sites for hydrogen atom storage.

The hydriding process of TiFe-based alloys can be divided into two stages, forming the β phase ($TiFeH_{1.04}$) and γ phase ($TiFeH_{1.95}$) respectively, and the structural distribution after generation can be seen in Figure 4. During this process, hydrogen atoms preferentially occupy the $[Ti_4Fe_2]$ octahedral interstitial sites. With increasing hydrogen content, hydrogen further occupies the $[Ti_2Fe_4]$ interstitial sites, resulting in unit cell volume expansion while the crystal structure still retains the CsCl-type characteristics.

The single-phase region of TiFe is relatively narrow, reaching its maximum width at the eutectic temperature of 1085 °C where the atomic fraction of Ti is only in the range of 49.7%–52.5%. Beyond this range, the alloy tends to form secondary phases such as $TiFe_2$. $TiFe_2$ is a C14 Laves phase, which does not react with hydrogen but can act as a hydrogen diffusion channel [78].

4.1.2 Hydrogen Storage Advantages and Intrinsic Problems of TiFe-Type CsCl Phase

The hydrogen storage advantages of the TiFe-type CsCl phase are significant. Its theoretical hydrogen storage capacity can reach 1.9 wt.%, and the equilibrium decomposition pressure at room temperature is approximately 0.3 MPa, which meets the requirements of hydrogen storage applications at room temperature and low pressure [80]. Meanwhile, owing to the abundant reserves and low cost of Fe, as well as the relatively sufficient reserves of Ti, TiFe-based alloys exhibit cost advantages in large-scale applications.

However, the TiFe-type CsCl phase has obvious intrinsic problems. It exhibits extremely poor oxidation resistance. When exposed to air, its surface readily reacts with O_2, H_2O and other substances to form a dense oxide film, resulting in alloy poisoning. The poisoned alloy requires repeated activation treatments at 400–450 °C and 5–6.5 MPa to absorb and desorb hydrogen, which greatly increases the application cost [81].

In addition, the hydrogen absorption and desorption process of TiFe alloy exhibits a two-plateau pressure phenomenon, with a large pressure difference between the two plateaus, which impairs the reversible hydrogen storage efficiency. Meanwhile, the alloy is prone to pulverization during cyclic hydrogen absorption and desorption, which further reduces its structural stability [82].

Studies have shown that the hydrogen storage performance of TiFe-based alloys is affected by Fe content. Alloys with a higher Fe content are more prone to forming an oxide layer on the surface, which reduces the hydrogen storage capacity and hydrogen absorption rate of the alloy. However, an appropriate amount of Fe doping can optimize the thermodynamics and kinetics of hydrogen storage in the alloy [83].

4.1.3 Hydrogen Storage Potential and Adaptability of CsCl-Type Phase in Ti-Based High-Entropy Systems

The core characteristics of high-entropy alloys are the coexistence of multiple principal elements and the high-entropy effect, which are well compatible

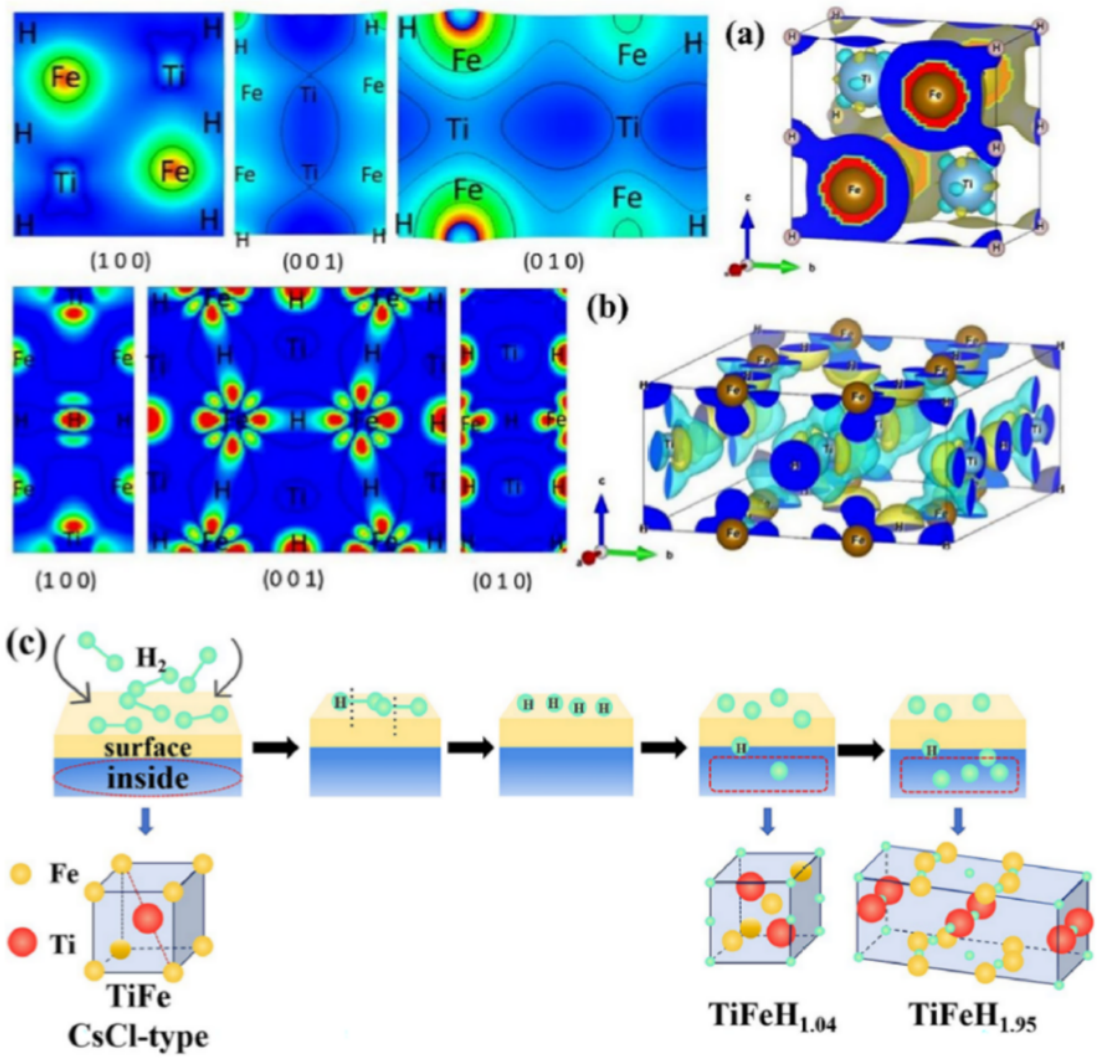

Figure 4. Charge density difference distribution diagram of (a) $TiFeH_{1.04}$, (b) $TiFeH_{1.95}$, and (c) hydrogen absorption diagram of TiFe hydrogen storage alloy [79].

with the hydrogen storage requirements of hydrogen storage alloys. The lattice distortion induced by the high-entropy effect can generate abundant micro-strains and defects in the alloy lattice. These defects can provide more sites for the adsorption, diffusion and nucleation of hydrogen atoms, thereby improving the hydrogen storage capacity and kinetic performance.

In Ti-based high-entropy alloys, the CsCl-type phase can form a synergistic effect with other phases. For example, when the CsCl-type phase is compounded with the BCC phase and the C14 Laves phase, the secondary phases can act as hydrogen diffusion channels and improve the activation performance of TiFe-based alloys. Such a multiphase synergistic effect can compensate for the intrinsic shortcomings of the single CsCl phase [79].

Furthermore, through high-entropy alloying design, various elements such as V, Zr, Mn and rare earth elements can be introduced into the TiFe-based CsCl-type phase. The synergistic effect of these elements can regulate the lattice parameters, interstitial size and electronic structure, thereby optimizing key properties including the hydrogen storage plateau pressure and activation energy, and fully exploiting the hydrogen storage potential of the CsCl-type phase [82].

In high-entropy alloys such as TiZrCrMnFeNi, the CsCl phase and C14 Laves phase coexist, enabling hydrogen absorption at room temperature without activation and achieving a hydrogen absorption capacity of 1.7 wt.% [23]. In Ti-V-Fe based alloys, doping with Fe promotes the formation of a multiphase structure consisting of a BCC main phase, C14 Laves secondary phase, and α-Ti secondary phase. These phases increase the phase boundary density, providing efficient channels for hydrogen diffusion

and improving hydrogen storage kinetics [83].

4.2 Experimental Progress on Hydrogen Storage of CsCl-Type Ti-Based Alloys

4.2.1 *Design and Preparation of Single-Phase CsCl-Type TiFe-Based Alloys*

The design of single-phase CsCl-type TiFe-based alloys requires strict control over composition and preparation processes. By adjusting the atomic ratios of Ti, Fe and other principal elements (such as V, Cr, Mn, Ni), combined with CALPHAD thermodynamic calculations, researchers can achieve the stable formation of a single-phase CsCl structure. For instance, the $Ti_{46}Fe_{47.5}V_{6.5}$ alloy forms a single-phase CsCl structure after vacuum arc melting through precise control of V content, with a room-temperature hydrogen storage capacity of up to 1.44 wt.% [82].

In terms of preparation, vacuum arc melting and induction melting are common methods. By repeated remelting and homogenization annealing (holding at 1000 °C for 4–8 h), composition segregation can be reduced and the formation of single-phase CsCl structure promoted [82]. In addition, mechanical alloying can refine grains to the nanoscale and introduce lattice defects, improving the activation performance of the alloy. However, excessive ball milling time leads to amorphization and reduces hydrogen storage capacity [79].

4.2.2 *Research Progress of Multiphase CsCl-Type TiFe-Based High-Entropy Alloys (CsCl+BCC/C14 Laves, etc.)*

The design focus of multiphase CsCl-type TiFe-based high-entropy alloys is to improve performance through multiphase synergy. The CsCl phase, as the main hydrogen storage phase, provides hydrogen storage capacity, while the BCC phase or C14 Laves phase serves as an auxiliary phase to improve activation kinetics. For example, in the TiZrCrMnFeNi high-entropy alloy, where the CsCl phase and C14 Laves phase coexist, hydrogen absorption can be achieved at room temperature without activation, with a hydrogen storage capacity of 1.7 wt.% [23]. Different multiphase combinations exhibit different performance advantages. In CsCl+BCC multiphase alloys, the high electrical conductivity and rapid hydrogen diffusion ability of the BCC phase can enhance hydrogen absorption and desorption kinetics. In CsCl+C14 Laves multiphase alloys, the Laves phase can inhibit alloy pulverization and improve cycling stability. For instance, in the $Ti_{1.08}Y_{0.02}Fe_{0.8}Mn_{0.2}Zr_{0.04}$ alloy composed of the CsCl phase and $ZrMn_2$ secondary phase, the hydrogen storage capacity reaches 1.6 wt.% at 303 K, and the incubation period is significantly shortened.

The preparation process of multiphase alloys needs to consider the formation conditions of each phase. The proportion and distribution of each phase can be regulated by controlling the cooling rate and heat treatment process. In addition, severe plastic deformation processes such as high-pressure torsion can refine the multiphase microstructure and introduce a large number of defects, further improving hydrogen storage performance. For example, the hydrogen storage capacity of the as-cast TiFe-based multiphase alloy increases from 0.2 wt.% to 2 wt.% at room temperature after high-pressure torsion treatment [85].

4.3 Hydrogen Storage Performance Regulation Strategies of TiFe-Based CsCl-Type High-Entropy Alloys

4.3.1 *Composition Design: Synergy of A/B Site Element Regulation and High-Entropy Effect*

Substitution of A-site (Ti-site) elements can effectively optimize hydrogen storage properties. After replacing Ti with elements such as Zr and V, the lattice parameters can be increased, expanding the interstitial sites for hydrogen storage and improving hydrogen storage capacity [86]. For example, in the $Ti_{49.87}Fe_{49.87}Zr_{0.26}$ alloy, although the addition of Zr does not change the hydrogen storage capacity, it significantly improves the activation performance [84, 87].

When rare-earth elements (La, Ce, Y) substitute Ti, dispersedly distributed secondary phases are formed. After hydrogen absorption, these phases undergo volume expansion and generate microcracks, which provide diffusion channels for hydrogen [79]. For instance, in the $Ti_{0.95}Y_{0.05}Fe_{0.8}Mn_{0.2}$ alloy, the addition of Y reduces the incubation period of the first hydrogen absorption from 73 min to 3 min.

Substitution of B-site (Fe-site) elements mainly improves kinetic and thermodynamic properties. Substitution of Fe with Mn or Cr can catalyze the dissociation of H_2 and enhance the activation rate. $TiFe_{0.85}Mn_{0.15}$ alloy can be reactivated by simple heat treatment after exposure to air [88]. And substitution of Fe with Ni or Co can reduce the slope of the hydrogen absorption plateau and improve the reversibility of hydrogen storage. However, excessive

substitution will lead to a decrease in hydrogen storage capacity [89].

The synergistic effect between the high-entropy effect and element substitution enables comprehensive optimization of properties. The mixing of multiple elements increases lattice distortion and defect density. Meanwhile, the functional complementarity of different elements not only enhances hydrogen storage capacity but also improves activation performance and cycling stability. For example, the TiZrFeMnCrV high-entropy alloy achieves a room-temperature hydrogen absorption capacity of 1.8 wt.% through multi-element synergistic regulation, with the capacity remaining at 1.76 wt.% after 50 cycles [90].

4.3.2 *Phase Structure Regulation: Synergy of Single-Phase Optimization and Multiphase Composite*

The optimization focus of single-phase CsCl-type alloys is to improve structural homogeneity. By precisely controlling composition and adopting homogenization annealing, lattice defects and elemental segregation can be reduced, thus optimizing the hydrogen storage plateau characteristics. For example, after homogenization annealing, the $TiFe_{0.9}Cr_{0.1}$ alloy exhibits a more stable hydrogen storage plateau pressure, with a deviation of only 0.022 MPa between the dehydrogenation pressure and the calculated value [82].

Multiphase composite regulation is the key to improving comprehensive performance. Reasonably designing the proportion of CsCl phase to BCC, C14 Laves and other phases can achieve complementary advantages. It should be noted that excessive introduction of secondary phases will reduce hydrogen storage capacity. For instance, the $V_{30}Ti_{30}Cr_{25}Fe_{10}Nb_5$ alloy shows a decreased hydrogen absorption rate due to excessive secondary phases [91].

Furthermore, precise regulation of phase structure can be achieved via fabrication processes. Techniques such as mechanical ball milling, cold rolling and high-pressure torsion can refine grains, promote the uniform and dispersed distribution of secondary phases, and simultaneously introduce abundant defects to accelerate hydrogen diffusion. This enables the synergistic effect of single-phase optimization and multiphase composite design, thereby improving the hydrogen storage performance of the alloy [77]. For example, TiFe multiphase alloys treated by high-pressure torsion can form a heterogeneous microstructure with coexisting nanocrystals, coarse grains and defects, leading to a significant improvement in hydrogen absorption capacity at room temperature [92].

4.3.3 *Surface and Catalytic Regulation: Passivation Layer Modification and Hydrogen Absorption–Desorption Kinetics Enhancement*

The surface passivation layer is the main obstacle affecting the activation performance of alloys. Mechanical ball milling can destroy the surface oxide film and expose fresh surfaces. Meanwhile, it refines particles and increases the specific surface area, thus improving hydrogen adsorption capacity. For example, after ball milling treatment, the hydrogen absorption capacity of TiFe alloy increases from 0.1 wt.% to 1.3 wt.% [92].

The addition of catalytic elements can significantly improve the hydrogen absorption and desorption kinetics. Transition metals such as Ni, Pd, and Pt exhibit excellent catalytic activity for H_2 dissociation. When compounded with TiFe-based alloys, they can accelerate the dissociation of hydrogen molecules into hydrogen atoms [93]. For example, after ball milling composite with Ni, the incubation period of TiFe alloy is only 12 s at 150 °C and 3 MPa [94]. Rare earth elements and their hydrides also exhibit catalytic effects. For instance, LaH_3, CeH_2 and others can promote hydrogen diffusion and improve activation performance.

Surface modification techniques can effectively enhance the anti-poisoning ability. Coating thin films of Pd, Ni and other materials on the alloy surface via vapor deposition and other methods can prevent the reaction of oxygen and water vapor with the matrix, while catalyzing hydrogen dissociation. For example, Pd-coated TiFe alloys can maintain good activation performance even after being exposed to air [95].

4.3.4 *Preparation Process Regulation: Control of Microstructure and Phase Structure*

Melting processes directly affect the phase structure and composition homogeneity of alloys.

Vacuum arc melting and induction melting can reduce oxygen contamination. Through repeated remelting and rapid cooling, the formation of harmful phases can be suppressed and the formation of the CsCl phase promoted [82]. For example, vacuum melting of the $TiFe_{0.8}Ni_{0.2}Co_m$ alloy under helium protection achieves uniform composition distribution and improves hydrogen storage stability [96].

Plastic deformation processes can significantly

optimize the microstructure. Processes such as cold rolling and high-pressure torsion can refine grains to the nanoscale and introduce high-density dislocations and microcracks, which provide fast channels for hydrogen diffusion. For instance, the TiFe alloy treated by high-pressure torsion can absorb hydrogen at room temperature without activation, with a hydrogen absorption capacity of 1.7 wt.% [86].

Heat treatment processes can regulate phase proportion and grain size. Homogenization annealing can eliminate composition segregation and promote the formation of single-phase CsCl structure; aging treatment can precipitate dispersed secondary phases and enhance the strengthening effect. For example, after annealing at 1000 °C for 8 h, 60%–80% of the C14 phase in the TiFeV alloy is dissolved, and both the hydrogen storage capacity and plateau characteristics are significantly improved [82].

5 Challenges and Perspectives

5.1 Ti-based Hydrogen storage alloys performance

According to relevant studies, the BCC lattice contains a large number of large-sized tetrahedral and octahedral interstices, which can accommodate a higher filling amount of hydrogen atoms, rendering it the phase with the maximum theoretical hydrogen storage capacity among the three types of phases.

The C14 Laves phase exhibits the optimal comprehensive performance in terms of reversible hydrogen storage, activation behavior and cycling stability. For many single-phase C14 alloys, the saturated hydrogen capacity is close to the reversible capacity, leading to a high capacity utilization rate. However, certain compositions, such as mechanically alloyed $Ti_{35}V_{35}Cr_5Mn_{20}Fe_5$, exhibit a significant disparity between absorption and reversible capacities, highlighting the critical influence of processing and phase stability on reversibility.

To date, no single-phase CsCl-type Ti-based high-entropy alloy has been reported to store hydrogen independently. Although conventional binary CsCl-type TiFe possesses theoretical hydrogen storage capability, the single-phase CsCl structure features highly ordered atomic arrangement and narrow interstices, accompanied by excessively strong metal-hydrogen bonding and an extremely high proportion of irreversible hydrogen. But CsCl-relevant alloys are under investigation. In multiphase high-entropy alloy systems, the CsCl phase mostly coexists as an auxiliary secondary phase with the C14 Laves phase. It assists hydrogen diffusion via the synergistic effect at the two-phase interface, yet cannot deliver effective hydrogen storage capacity on its own, for instance, TiZrCrMnFeNi achieves hydrogen storage through the combined action of the C14 Laves phase and the CsCl-type structure. And the hydrogen storage properties of representative Ti-based high-entropy alloys with the above three structures are summarized in Table 1.

5.2 Challenges

Ti- and Zr-containing alloys easily generate dense passivating oxide layers on their surfaces, which demand rigorous pre-activation treatment. Their hydrogen absorption performance will degrade sharply after long-term exposure to air, and currently available surface modification approaches are costly and cannot sustain long-term effectiveness. There is an unavoidable trade-off between hydrogen storage capacity and reversible performance. Single-phase BCC alloys feature high theoretical capacity but fail to release hydrogen completely at room temperature, whereas C14 Laves and CsCl-type phases exhibit fast sorption kinetics with limited maximum storage capacity. Even dual-phase composites cannot maintain

Table 1. Hydrogen storage performances of representative Ti-based high-entropy alloys with BCC phase, C14 Laves phase and CsCl-Type structures.

	Composition	Synthesis and processing	H_2 absorp. capacity	Rev.H_2 capacity	Plateau pressure	Activation performance	Cyclic stability	Ref.
BCC	TiZrNbTa	vacuum arc remelting	1.67wt%	N/A	1.6 MPa	Hydrogenation activation energy: 6.14kJ/mol	Capacity dropped from 1.6 wt% to 1.38 wt% after 10 cycles	[53]
	TiZrHfNbTa	vacuum arc remelting	D/M=1.918 (3.13 wt%)	2.54wt%	N/A	Absorption: 12.2kJ/mol; desorption: 11.9kJ/mol	The capacity exhibits almost no decay after 10 cycles.	[52]
C14 Laves	TiZrCrFeMnNi	vacuum arc remelting	S53:1.493 wt%: S200:1.539 wt%	S53: 1.41 wt%; S200 1.46 wt%	S53: Absorption: 1.325 MPa, desorption: 0.795 MPa; S200: Absorption: 1.317 MPa, desorption: 0.779 MPa	N/A	Both samples display marginal capacity reduction after 5 activation cycles.	[24]
	$Ti_{35}V_{35}Cr_5Mn_{20}Fe_5$	vacuum arc remelting	1.39wt%	0.40wt%	N/A	Absorption Stage I: 12.15 kJ/mol Absorption Stage II: 15.05 kJ/mol Desorption: -19.93 kJ/mol	No prominent capacity degradation occurs.	[44]
CsCl-relevant alloys	TiZrCrMnFeNi	arc melting	1.7 wt%	1.7wt%	3.9 MPa	No activation required	The capacity decay is extremely low.	[23]
	TiVCrFeZr	vacuum arc remelting	2.27 wt%	1.04 wt%	N/A	N/A	Marked capacity degradation after five cycles	[33]

a stable balance of the two advantages throughout repeated cycles, and ongoing lattice distortion and material pulverization steadily cut down reversible capacity. In terms of large-scale industrialization, raw materials such as vanadium and niobium bring high costs, while fabrication methods like high-pressure torsion and laser additive manufacturing remain confined to laboratory usage. Bulk ingots suffer from elemental volatilization and compositional segregation, leading to inconsistent performance among samples, and hydrogen embrittlement further shortens the service life of alloys in practical hydrogen storage devices.

5.3 Perspectives

Low-cost rare-earth doping and non-noble metal thin catalytic coatings might be adopted to alleviate surface passivation, enabling direct hydrogen uptake at room temperature without high-temperature pre-treatment. Multiphase microstructures will be precisely optimized with the guidance of valence electron concentration, mixing enthalpy and DFT simulation data to weaken metal-hydrogen bonding and boost room-temperature reversible capacity. Researchers might also develop cheap raw material systems and scalable manufacturing technologies including large-scale mechanical alloying and continuous melting, alongside matched forming and heat treatment procedures to mitigate segregation and hydrogen embrittlement for industrial application. Meanwhile, operando characterization technologies and machine learning frameworks will be integrated to uncover dynamic hydrogenation phase transition mechanisms and speed up the screening of alloys suitable for practical hydrogen storage conditions.

6 Conclusion

In summary, Ti-based high-entropy alloys (HEAs) represent a paradigm shift in solid-state hydrogen storage, overcoming the inherent limitations of conventional intermetallics through compositional complexity and tailored microstructures. A central insight of this review is that no single-phase configuration satisfies all practical requirements simultaneously; instead, optimal performance is achieved via multiphase architectural design. This approach strategically balances the high capacity of BCC phases, the rapid kinetics and catalytic activity of C14 Laves phases, and the cost-effectiveness and favorable thermodynamics of CsCl-type phases. Guided by empirical descriptors and powered by computational tools such as CALPHAD, DFT, and machine learning, the field is transitioning from empirical trial-and-error toward rational alloy design.

Despite significant progress, several critical challenges persist. These include the fundamental trade-off between gravimetric capacity and reversible dehydrogenation in BCC-dominated systems, surface passivation hindering initial activation, and hydrogen-induced embrittlement affecting long-term cyclic stability. Furthermore, the scalability of synthesis routes and the economic viability of constituent elements remain pivotal for commercial translation.

Future advancements should prioritize the integration of high-throughput experimentation with machine learning to accelerate compositional discovery. Complementary insights from operando characterization techniques, including in situ synchrotron XRD and neutron scattering, are essential to elucidate phase transformation dynamics and hydrogen diffusion pathways under service conditions. By establishing robust process-structure-property relationships, Ti-based HEAs are poised to evolve from laboratory curiosities into viable solutions for next-generation hydrogen storage and related energy applications.

Data Availability Statement

Not applicable.

Funding

This work was supported by the National Key Research and Development Program of China under Grant 2023YFB4005402, and by the National Natural Science Foundation of China under Grant NSFC-NSAF, U2330111.

Conflicts of Interest

The authors declare no conflicts of interest.

AI Use Statement

The authors declare that no generative AI was used in the preparation of this manuscript.

Ethical Approval and Consent to Participate

Not applicable.

References

[1] Hu, H. Z., Zhang, X. X., Li, S. S., Yi, L. C., & Chen, Q. J. (2024). A review of body-centered cubic-structured alloys for hydrogen storage: composition, structure, and properties. *Rare Metals, 44*(3), 1497–1521. [CrossRef]

[2] Hu, H. Z., Xiao, H. Q., He, X. C., Zhou, W. H., Zhang, X. X., Tang, R. Z., ... & Chen, Q. J. (2024). Development of Ti–V–Cr–Mn–Mo–Ce high-entropy alloys for high-density hydrogen storage in water bath environments. *Rare Metals, 43*(10), 5229-5241. [CrossRef]

[3] Hu, J., Zhang, J., Xiao, H., Xie, L., Sun, G., Shen, H., ... & Zu, X. (2021). A first-principles study of hydrogen storage of high entropy alloy TiZrVMoNb. *International Journal of Hydrogen Energy, 46*(40), 21050-21058. [CrossRef]

[4] Kamble, A., Sharma, P., & Huot, J. (2020). Effect of heat treatment on crystal structure, microstructure, and hydrogenation behavior of BCC 52Ti-12V-36Cr alloys with Zr and Zr-Ni additives. *Metallurgical and Materials Transactions A, 51*(4), 1945-1952. [CrossRef]

[5] Gao, Y., Yin, D., Li, Y., Luo, L., Ding, N., Wang, Z., ... & Cheng, Y. (2024). Composition optimization and hydrogen storage properties of Ti–V–Mn–Fe alloys. *International Journal of Hydrogen Energy, 51*, 88-97. [CrossRef]

[6] Wei, M., Liu, Y., Xing, X., Zhang, Z., & Liu, T. (2023). (TiVZrNb) 83Cr17 high-entropy alloy as catalyst for hydrogen storage in MgH2. *Chemical Engineering Journal, 476*, 146639. [CrossRef]

[7] Serrano, L. B., Moussa, M., Yao, J. Y., Silva, G., Bobet, J. L., Ferreira, S. S., & Kátia, R. (2023). Development of Ti-V-Nb-Cr-Mn high entropy alloys for hydrogen storage. *Journal of Alloys and Compounds, 945*, 169289. [CrossRef]

[8] Zhai, Y. T., Li, Y. M., Bolzoni, L., Kennedy, J., & Yang, F. (2024). Effect of heat treatment on microstructural evolution and hydrogen storage performance of as-milled Ti5+xV35(CrMnFe)60-x (x=0, 10, 20, 30) high-entropy alloys. *International Journal of Hydrogen Energy, 81*, 584–594. [CrossRef]

[9] Kumar, A., Yadav, T. P., Shaz, M. A., & Mukhopadhyay, N. K. (2024). Hydrogen storage properties in rapidly solidified TiZrVCrNi high-entropy alloys. *Energy Storage, 6*(1), e532. [CrossRef]

[10] Park, K. B., Park, J. Y., Kim, Y. D., Fadonougbo, J. O., Kim, S., Kim, H. K., ... & Park, H. K. (2022). Characterizations of hydrogen absorption and surface properties of Ti0. 2Zr0. 2Nb0. 2V0. 2Cr0. 17Fe0. 03 high entropy alloy with dual phases. *Metals and Materials International, 28*(2), 565-571. [CrossRef]

[11] Cao, Z. M., Zhou, P. P., Xiao, X. Z., Zhan, L. J., Jiang, Z. F., Wang, S. M., ... & Chen, L. X. (2022). Development of Ti0. 85Zr0. 17 (Cr-Mn-V) 1.3 Fe0. 7-based Laves phase alloys for thermal hydrogen compression at mild operating temperatures. *Rare Metals, 41*(8), 2588-2594. [CrossRef]

[12] Ma, X. F., Ding, X., Liu, E. L., Chen, R. R., Wang, X. X., Zhang, Y., & Guo, J. J. (2024). Modification of BCC phase and the enhanced reversible hydrogen storage properties of Ti-V-Fe-Mn alloys with varied V/Fe ratios. *China Foundry, 21*(5), 546-554. [CrossRef]

[13] Zhao, Y., Cai, H., Cao, Y., Zhang, Y., Xu, D., Wang, H., ... & Xue, Y. (2025). Improved dynamic performance of Ni-doped Ti–Cr–Mo BCC alloys for hydrogen storage at ambient temperature. *Journal of Materials Science, 60*(32), 14048-14056. [CrossRef]

[14] Kao, Y. F., Chen, S. K., Sheu, J. H., Lin, J. T., Lin, W. E., Yeh, J. W., ... & Wang, C. W. (2010). Hydrogen storage properties of multi-principal-component CoFeMnTixVyZrz alloys. *International Journal of Hydrogen Energy, 35*(17), 9046-9059. [CrossRef]

[15] Mishra, S. S., Mukhopadhyay, S., Yadav, T. P., Mukhopadhyay, N. K., & Srivastava, O. N. (2019). Synthesis and characterization of hexanary Ti–Zr–V–Cr–Ni–Fe high-entropy Laves phase. *Journal of Materials Research, 34*(5), 807-818. [CrossRef]

[16] Cheng, B., Li, Y., Li, X., Ke, H., Wang, L., Cao, T., ... & Xue, Y. (2023). Solid-state hydrogen storage properties of Ti–V–Nb–Cr high-entropy alloys and the associated effects of transitional metals (M= Mn, Fe, Ni). *Acta Metallurgica Sinica (English Letters), 36*(7), 1113-1122. [CrossRef]

[17] Edalati, P., Andrade, G., Strozi, R. B., Dangwal, S., Edalati, K., & Floriano, R. (2025). Room temperature hydrogen storage properties of Ti-Zr-Mn-Fe-Co high-entropy alloys designed by semi-empirical descriptors, thermodynamic calculations and machine learning. *Journal of Alloys and Compounds, 1022*, 180051. [CrossRef]

[18] Floriano, R., Zepon, G., Edalati, K., Fontana, G. L., Mohammadi, A., Ma, Z., ... & Contieri, R. J. (2020). Hydrogen storage in TiZrNbFeNi high entropy alloys, designed by thermodynamic calculations. *International Journal of Hydrogen Energy, 45*(58), 33759-33770. [CrossRef]

[19] Hu, J., Zhang, J., Xiao, H., Xie, L., Sun, G., Shen, H., ... & Zu, X. (2021). The effect of hydrogen on the mechanical properties of high entropy alloy TiZrHfMoNb: First-principles investigation. *Journal of Alloys and Compounds, 879*, 160482. [CrossRef]

[20] Singh, A., Kumari, P., Sahoo, S. K., & Shahi, R. R. (2025). Studies on hydrogen storage properties of TiVFeNi,(TiVFeNi) 95Zr5 and (TiVFeNi) 90Zr10 high entropy alloys. *International Journal of Hydrogen Energy, 141*, 738-749. [CrossRef]

[21] Zhu, Y., Yang, X. S., Xu, Z. L., Tsui, G. C. P., Zhou, Q., Tang, R., ... & Chan, K. (2024). Development of AB2-type TiZrCrMnFeCoV intermetallic high-entropy alloy for reversible room-temperature hydrogen storage. *Journal of Energy Storage, 75*, 109553.

[CrossRef]

[22] Dangwal, S., & Edalati, K. (2024). High-entropy alloy TiV2ZrCrMnFeNi for hydrogen storage at room temperature with full reversibility and good activation. *Scripta Materialia, 238*, 115774. [CrossRef]

[23] Edalati, P., Floriano, R., Mohammadi, A., Li, Y., Zepon, G., Li, H. W., & Edalati, K. (2020). Reversible room temperature hydrogen storage in high-entropy alloy TiZrCrMnFeNi. *Scripta Materialia, 178*, 387-390. [CrossRef]

[24] Ha, H., Jung, S. J., Jeong, S. G., Kim, R. E., Park, H. K., & Kim, H. S. (2025). Enhancing hydrogen storage kinetics and capacity via particle size modulation in TiZrCrFeMnNi high-entropy alloy. *International Journal of Hydrogen Energy, 99*, 1047-1054. [CrossRef]

[25] Lee, H., Dewangan, S. K., Sharma, A., & Ahn, B. (2025). Initial hydrogenation in multiphase TiFeCoNiCu high-entropy alloy for hydrogen storage. *Journal of Alloys and Compounds, 1022*, 179711. [CrossRef]

[26] Chen, J., Xu, T., Zhang, J., Huang, H., Yuan, J., Liu, B., ... & Wu, Y. (2024). Improving the plateau performance of the TiZrFeMnCrV high-entropy alloy by partial substitution of V with Fe, Mn and Cr. *Materials Chemistry and Physics, 318*, 129219. [CrossRef]

[27] Enblom, V., Clulow, R., Ha, T. J., Witman, M. D., Way, L. E., Han, S. J., ... & Fadonougbo, J. O. (2025). A combined experimental and machine learning exploration of Ti2-xZrxMnCrFeNi high entropy Laves hydrides. *Materialia, 40*, 102414. [CrossRef]

[28] Shen, H., Hu, J., Li, P., Huang, G., Zhang, J., Zhang, J., ... & Peng, S. (2020). Compositional dependence of hydrogenation performance of Ti-Zr-Hf-Mo-Nb high-entropy alloys for hydrogen/tritium storage. *Journal of Materials Science & Technology, 55*, 116-125. [CrossRef]

[29] Vicente, I. S., Andrade, G., Silva, B. H., Ponsoni, J. B., Dias, J. A., Zepon, G., ... & Floriano, R. (2025). Exploring the Dual-Phase Configuration of Multicomponent Alloys in the Ti21Zr21V x Fe y Ni z (x+ y+ z= 58 at%) System for Room Temperature Hydrogen Storage. *Energy & Fuels, 39*(33), 15888-15902. [CrossRef]

[30] Andrade, G., Huot, J., & Floriano, R. (2025). Microstructural evolution and hydrogen storage performance of TiZrHfVNb1-xCux (for X = 0, 0.6, 0.8 and 1) high-entropy alloys. *Materials Chemistry and Physics, 343*, 131069. [CrossRef]

[31] Savvotin, I., Berdonosova, E., Korol, A., Zadorozhnyy, V., Zadorozhnyy, M., Bazlov, A., ... & Klyamkin, S. (2024). Evaluation of hydrogen storage performance of Ti0. 25Zr0. 25V0. 15Nb0. 15Ta0. 2 high-entropy alloy using calorimetric technique. *Journal of Alloys and Compounds, 1005*, 176022. [CrossRef]

[32] Liu, J., Xu, J., Sleiman, S., Chen, X., Zhu, S., Cheng, H., & Huot, J. (2021). Microstructure and hydrogen storage properties of Ti–V–Cr based BCC-type high entropy alloys. *International Journal of Hydrogen Energy, 46*(56), 28709-28718. [CrossRef]

[33] Zareipour, F., Shahmir, H., Huang, Y., Patel, A. K., Dematteis, E. M., & Baricco, M. (2024). Hydrogen storage in TiVCr (Fe, Co)(Zr, Ta) multi-phase high-entropy alloys. *International Journal of Hydrogen Energy, 94*, 639-649. [CrossRef]

[34] Liang, J., Li, G., Ding, X., Li, Y., Wen, Z., Zhang, T., & Qu, Y. (2024). The synergistic effect of Ni and C14 Laves phase on the hydrogen storage properties of TiVZrNbNi high entropy hydrogen storage alloy. *Intermetallics, 164*, 108102. [CrossRef]

[35] Liang, J., Li, G., Ding, X., Li, Y., Wen, Z., Zhang, T., & Qu, Y. (2023). Effect of C14 Laves/BCC on microstructure and hydrogen storage properties of (Ti32. 5V27. 5Zr7. 5Nb32. 5) 1-xFex (x= 0.03, 0.06, 0.09) high entropy hydrogen storage alloys. *Journal of Energy Storage, 73*, 108852. [CrossRef]

[36] Wen, Z., Li, G., Wang, S., Li, Y., Zhang, T., Ding, X., & Qu, Y. (2025). Effect of Zr content on hydrogen absorption and desorption properties of Ti35-xV25Cr15Nb25Zrx (x= 0, 2, 4, 6, 8) high entropy alloys. *International Journal of Hydrogen Energy, 175*, 151468. [CrossRef]

[37] Wang, J., Zhou, P., Jia, Y., Feng, J., Qi, J., Chu, F., ... & Xiao, X. (2024). Binding energy crossover mechanism enables low-temperature hydrogen storage performance of dual-phase TiZrCrMnNi (VFe) high-entropy alloy. *Chemical Engineering Journal, 502*, 157871. [CrossRef]

[38] Chen, J., Huang, H., Xu, T., Lv, Y., Liu, B., Zhang, B., ... & Wu, Y. (2024). Enhancement of vanadium addition on hydrogen storage properties of high entropy alloys TiZrFeMnCrVx. *International Journal of Hydrogen Energy, 50*, 1223-1233. [CrossRef]

[39] Hidalgo-Jimenez, J., Cubero-Sesin, J. M., Edalati, K., Khajavi, S., & Huot, J. (2023). Effect of high-pressure torsion on first hydrogenation of Laves phase Ti0. 5Zr0. 5 (Mn1-xFex) Cr1 (x= 0, 0.2 and 0.4) high entropy alloys. *Journal of Alloys and Compounds, 969*, 172243. [CrossRef]

[40] Cheng, B., Dou, B., Kong, L., Wan, D., & Xue, Y. (2025). Synergistic and Competing Effects of Iron in TiVNbCr-Based High-Entropy Alloys for Reversible Hydrogen Storage. *Small, 21*(44), e08310. [CrossRef]

[41] Hu, J., Zhang, J., Xiao, H., Xie, L., Shen, H., Li, P., ... & Zu, X. (2020). A density functional theory study of the hydrogen absorption in high entropy alloy TiZrHfMoNb. *Inorganic Chemistry, 59*(14), 9774-9782. [CrossRef]

[42] Montero, J., Ek, G., Laversenne, L., Nassif, V., Zepon, G., Sahlberg, M., & Zlotea, C. (2020). Hydrogen storage properties of the refractory Ti–V–Zr–Nb–Ta multi-principal element alloy. *Journal of Alloys and Compounds, 835*, 155376. [CrossRef]

[43] Andrade, G., Zepon, G., Edalati, K., Mohammadi,

A., Ma, Z., Li, H. W., & Floriano, R. (2023). Crystal structure and hydrogen storage properties of AB-type TiZrNbCrFeNi high-entropy alloy. *International Journal of Hydrogen Energy, 48*(36), 13555-13565. [CrossRef]

[44] Zhai, Y. T., Li, Y. M., Liu, Z. C., Bolzoni, L., Kennedy, J., & Yang, F. (2025). Hydrogen ab/desorption behavior of the mechanical alloyed Ti–V–Cr–Mn–Fe HEAs with varying Mn/Cr ratio. *International Journal of Hydrogen Energy, 109*, 1008-1022. [CrossRef]

[45] Kumar, A., Yadav, T. P., Shaz, M. A., & Mukhopadhyay, N. K. (2024). Hydrogen storage performance of C14 type Ti0. 24V0. 17Zr0. 17Mn0. 17Co0. 17Fe0. 08 high entropy intermetallics. *Transactions of the Indian National Academy of Engineering, 9*(3), 585-593. [CrossRef]

[46] Kunce, I., Polanski, M., & Bystrzycki, J. (2014). Microstructure and hydrogen storage properties of a TiZrNbMoV high entropy alloy synthesized using Laser Engineered Net Shaping (LENS). *International Journal of Hydrogen Energy, 39*(18), 9904-9910. [CrossRef]

[47] Tau, J., Siyasiya, C., Modiba, R., Mathe, N., Arthur, N., & Pityana, S. (2024). Investigation of hydrogen storage properties for high entropy alloys (Ti30V30Cr30Fe10 and Ti40V30Cr10Fe10Al10). In *MATEC Web of Conferences* (Vol. 406, p. 06008). EDP Sciences. [CrossRef]

[48] Kawasuso, A., Arashima, H., Maekawa, M., Itoh, H., & Kabutomori, T. (2009). TiCrV hydrogen storage alloy studied by positron annihilation spectroscopy. *Journal of alloys and compounds, 486*(1-2), 278-283. [CrossRef]

[49] Rousselot, S., Guay, D., & Roué, L. (2010). Synthesis of fcc Mg–Ti–H alloys by high energy ball milling: Structure and electrochemical hydrogen storage properties. *Journal of Power Sources, 195*(13), 4370-4374. [CrossRef]

[50] Dou, T., Wu, Z., Mao, J., & Xu, N. (2008). Application of commercial ferrovanadium to reduce cost of Ti–V-based BCC phase hydrogen storage alloys. *Materials Science and Engineering: A, 476*(1-2), 34-38. [CrossRef]

[51] Young, K., Ouchi, T., Nei, J., & Meng, T. (2015). Effects of Cr, Zr, V, Mn, Fe, and Co to the hydride properties of Laves phase-related body-centered-cubic solid solution alloys. *Journal of Power Sources, 281*, 164-172. [CrossRef]

[52] Chen, Z., Zhang, S., Jiang, X., Zheng, M., Yang, H., Sun, Y., & Li, G. (2025). Properties and applications of deuterium absorption-desorption in TiZrHfNbTa high entropy alloy. *Journal of Nuclear Materials, 615*, 155987. [CrossRef]

[53] Zhang, C., Song, A., Yuan, Y., Wu, Y., Zhang, P., Lu, Z., & Song, X. (2020). Study on the hydrogen storage properties of a TiZrNbTa high entropy alloy. *International Journal of Hydrogen Energy, 45*(8), 5367-5374. [CrossRef]

[54] Sleiman, S., & Huot, J. (2021). Effect of particle size, pressure and temperature on the activation process of hydrogen absorption in TiVZrHfNb high entropy alloy. *Journal of Alloys and Compounds, 861*, 158615. [CrossRef]

[55] Zhu, Y., Li, X., Yang, X. S., Chen, P., Tsui, G. C. P., Xu, Z. L., ... & Chan, K. (2023). Compositionally complex doping for low-V Ti-Cr-V hydrogen storage alloys. *Chemical Engineering Journal, 477*, 146970. [CrossRef]

[56] Jeyaraman, S., Danilov, D. L., Notten, P. H., Ragula, U. B. R., Ramalingam, V. V., & Manivasagam, T. G. (2025). Influence of Ni and Nb addition in TiVCr-based high entropy alloys for room-temperature hydrogen storage. *Energies, 18*(15), 3920. [CrossRef]

[57] Martínez, A., & Santos, D. D. (2012). Hydrogen absorption/desorption properties in the TiCrV based alloys. *Materials Research, 15*(5), 809-812. [CrossRef]

[58] Wang, L., Zhang, L., Lu, X., Wu, F., Sun, X., Zhao, H., & Li, Q. (2023). Surprising cocktail effect in high entropy alloys on catalyzing magnesium hydride for solid-state hydrogen storage. *Chemical Engineering Journal, 465*, 142766. [CrossRef]

[59] Strozi, R. B., Leiva, D. R., Huot, J., Botta, W. J., & Zepon, G. (2021). Synthesis and hydrogen storage behavior of Mg–V–Al–Cr–Ni high entropy alloys. *International Journal of Hydrogen Energy, 46*(2), 2351-2361. [CrossRef]

[60] Feng, R., Liaw, P. K., Gao, M. C., & Widom, M. (2017). First-principles prediction of high-entropy-alloy stability. *npj Computational Materials, 3*(1), 50. [CrossRef]

[61] Marques, F., Balcerzak, M., Winkelmann, F., Zepon, G., & Felderhoff, M. (2021). Review and outlook on high-entropy alloys for hydrogen storage. *Energy & Environmental Science, 14*(10), 5191-5227. [CrossRef]

[62] Pedroso, O. A., Botta, W. J., & Zepon, G. (2022). An open-source code to calculate pressure-composition-temperature diagrams of multicomponent alloys for hydrogen storage. *International Journal of Hydrogen Energy, 47*(76), 32582-32593. [CrossRef]

[63] Zlotea, C., Sow, M. A., Ek, G., Couzinié, J. P., Perrière, L., Guillot, I., ... & Sahlberg, M. (2019). Hydrogen sorption in TiZrNbHfTa high entropy alloy. *Journal of Alloys and Compounds, 775*, 667-674. [CrossRef]

[64] Kong, L., Cheng, B., Wan, D., & Xue, Y. (2023). A review on BCC-structured high-entropy alloys for hydrogen storage. *Frontiers in Materials, 10*, 1135864. [CrossRef]

[65] Yu, C. S., Ma, C. Y., Zheng, W. S., He, Y. L., Wang, J., Yuan, G., ... & Lu, X. G. (2025). Experimental investigation and thermodynamic modeling of Ti–V–Fe–Mn hydrogen storage alloy system. *Journal of Iron and Steel Research International, 32*(11), 4038-4051. [CrossRef]

[66] Nygård, M. M., Ek, G., Karlsson, D., Sørby, M. H.,

Sahlberg, M., & Hauback, B. C. (2019). Counting electrons-a new approach to tailor the hydrogen sorption properties of high-entropy alloys. *Acta Materialia, 175*, 121-129. [CrossRef]

[67] Zlotea, C., Bouzidi, A., Montero, J., Ek, G., & Sahlberg, M. (2022). Compositional effects on the hydrogen storage properties in a series of refractory high entropy alloys. *Frontiers in Energy Research, 10*, 991447. [CrossRef]

[68] Zepon, G., Leiva, D. R., Strozi, R. B., Bedoch, A., Figueroa, S. J. A., Ishikawa, T. T., & Botta, W. J. (2018). Hydrogen-induced phase transition of MgZrTiFe0. 5Co0. 5Ni0. 5 high entropy alloy. *International Journal of Hydrogen Energy, 43*(3), 1702-1708. [CrossRef]

[69] Savvotin, I., Berdonosova, E., Korol, A., Zadorozhnyy, V., Zadorozhnyy, M., Statnik, E., ... & Klyamkin, S. (2023). Thermochemical analysis of hydrogenation of Pd-containing composite based on TiZrVNbTa high-entropy alloy. *Applied Sciences, 13*(16), 9052. [CrossRef]

[70] Sahlberg, M., Karlsson, D., Zlotea, C., & Jansson, U. (2016). Superior hydrogen storage in high entropy alloys. *Scientific reports, 6*(1), 36770. [CrossRef]

[71] Park, K. B., Park, J. Y., Do Kim, Y., Choi, J. I., Im, H. T., Kang, J. W., ... & Park, H. K. (2021). Study on hydrogen absorption and surface properties of TiZrVNbCr high entropy alloy. *Intermetallics, 130*, 107074. [CrossRef]

[72] Bobet, J. L., & Darriet, B. (2000). Relationship between hydrogen sorption properties and crystallography for TiMn2 based alloys. *International journal of hydrogen energy, 25*(8), 767-772. [CrossRef]

[73] Zhou, D., Zheng, C., Zhao, D., Guo, S., Li, J., Cao, Z., & Zhang, Y. (2025). Structure, modification and application of TiMn2-based hydrogen storage alloys. *Journal of Alloys and Compounds*, 182266. [CrossRef]

[74] Pan, Q., Shen, H., Han, X., Zhu, J., Li, Z., Pan, T., ... & Lv, L. (2025). Effect of non-stoichiometric Mn and Cr on the hydrogen storage properties of Ti–Mn-based alloys. *RSC advances, 15*(22), 17153-17163. [CrossRef]

[75] Serrano, L. B., Moussa, M., Silva, G., Santos, S. F., Bobet, J. L., & Cardoso, K. R. (2026). Effect of Laves phase on hydrogen storage properties of BCC Ti-V-Nb–Cr–Mn high entropy alloys. *Materials Science and Engineering: A*, 149936. [CrossRef]

[76] Tsoumou, G. C., & Huot, J. (2026). Synergy between BCC and C14 phases on the hydrogenation properties of the two phases high-entropy alloy Ti16Zr4V35Cr15Ni10Mn20. *International Journal of Hydrogen Energy, 206*, 153384. [CrossRef]

[77] Li, Y., Zhang, Y., Shang, H., Gao, J., Zhang, W., & Ju, L. (2023). Hydrogen storage characteristics of Ti1. 04Fe0. 7Ni0. 1Zr0. 1Mn0. 1Pr0. 06 alloy treated by ball milling. *Journal of Alloys and Compounds, 930*, 167024. [CrossRef]

[78] Gosselin, C., Santos, D., & Huot, J. (2017). First hydrogenation enhancement in TiFe alloys for hydrogen storage. *Journal of Physics D: Applied Physics, 50*(37), 375303. [CrossRef]

[79] Niu, Y., Li, T., Yuan, Z., Han, Q., Han, Z., Liu, C., & Sun, Y. (2025). An overview of TiFe-based alloys for hydrogen storage: structure, element substitution and preparation. *International Journal of Hydrogen Energy, 175*, 151503. [CrossRef]

[80] Liu, H., Zhang, J., Sun, P., Zhou, C., Liu, Y., & Fang, Z. Z. (2022). Effect of oxygen on the hydrogen storage properties of TiFe alloys. *Journal of Energy Storage, 55*, 105543. [CrossRef]

[81] Sandrock, G. (1999). A panoramic overview of hydrogen storage alloys from a gas reaction point of view. *Journal of alloys and compounds, 293*, 877-888. [CrossRef]

[82] Padhee, S. P., Sakaki, K., Shukla, V., Hwang, K., Cho, Y. W., & Lee, Y. S. (2025). Optimizing hydrogen storage in TiFe–V alloys: influence of sample purity and heat treatment. *International Journal of Hydrogen Energy, 138*, 874-883. [CrossRef]

[83] Wu, G., Xia, S., Cai, H., Jiang, J., Li, X., Li, R., ... & Wang, X. (2026). Insights into the role of Fe in modulating the microstructure, hydrogen storage properties and thermodynamic properties of Ti–V based alloys. *International Journal of Hydrogen Energy, 210*, 153602. [CrossRef]

[84] Gosselin, C., & Huot, J. (2015). Hydrogenation properties of TiFe doped with zirconium. *Materials, 8*(11), 7864-7872. [CrossRef]

[85] Kwak, R. H., Jung, S., Park, T. Y., Park, S. M., & Park, H. K. (2025). Microstructural feature and hydrogen storage properties of TiFe0. 7Mn0. 2X0. 1 (X= V, Cr, Co, Ni, Cu) hydrogen storage alloy. *International Journal of Hydrogen Energy, 113*, 485-494. [CrossRef]

[86] Ma, X., Ding, X., Hu, S., Zhao, Y., Wang, Q., Zhang, Y., ... & Chen, R. (2025). Fast reaction behaviors of AB-type Ti-Fe-Mn hydrogen storage alloys from lattice modification and in-situ formed yttrium hydride. *Chemical Engineering Journal, 507*, 160801. [CrossRef]

[87] Endo, N., Suzuki, S., Goshome, K., & Maeda, T. (2017). Operation of a bench-scale TiFe-based alloy tank under mild conditions for low-cost stationary hydrogen storage. *International journal of hydrogen energy, 42*(8), 5246-5251. [CrossRef]

[88] Ko, W. S., Park, K. B., & Park, H. K. (2021). Density functional theory study on the role of ternary alloying elements in TiFe-based hydrogen storage alloys. *Journal of Materials Science & Technology, 92*, 148-158. [CrossRef]

[89] Liu, H., Zhang, J., Sun, P., Zhou, C., Liu, Y., & Fang, Z. Z. (2023). An overview of TiFe alloys for hydrogen storage: Structure, processes, properties, and applications. *Journal of Energy Storage, 68*, 107772. [CrossRef]

[90] Fadonougbo, J. O., Park, K. B., Na, T. W., Park, C. S., Park, H. K., & Ko, W. S. (2022). An

integrated computational and experimental method for predicting hydrogen plateau pressures of TiFe1-xMx-based room temperature hydrides. *İnternational journal of hydrogen energy, 47*(40), 17673-17682. [CrossRef]

[91] Shang, H., Sheng, P., Li, J., Zhang, W., Zhang, X., Guo, S., ... & Zhang, Y. (2024). Characteristics of hydrogen storage of as-milled TiFe-based alloys. *International Journal of Hydrogen Energy, 50*, 190-200. [CrossRef]

[92] Han, Z., Wang, B., Zhai, T., Sun, H., Li, T., Yuan, Z., ... & Zhang, Y. (2025). Influence on the microstructure and hydrogen storage properties of Y–TiFe-based composites with transition metals via mechanical milling. *Intermetallics, 177*, 108603. [CrossRef]

[93] Zhang, X., Li, B., Wang, L., Xiong, W., Li, J., Zhou, S., ... & Yan, H. (2024). Hydrogen storage properties of AB2 type Ti–Zr–Cr–Mn–Fe based alloys. *International Journal of Hydrogen Energy, 51*, 193-201. [CrossRef]

[94] Nayebossadri, S., Greenwood, C. J., & Book, D. (2023). Evaluating some design criteria for TiFe-based ternary hydrogen storage alloys. *Journal of Alloys and Compounds, 947*, 169456. [CrossRef]

[95] Jain, P., Gosselin, C., & Huot, J. (2015). Effect of Zr, Ni and Zr7Ni10 alloy on hydrogen storage characteristics of TiFe alloy. *International Journal of Hydrogen Energy, 40*(47), 16921-16927. [CrossRef]

[96] Padhee, S. P., Roy, A., & Pati, S. (2021). Mechanistic insights into efficient reversible hydrogen storage in ferrotitanium. *International Journal of Hydrogen Energy, 46*(1), 906-921. [CrossRef]